Renewable and Sustainable Energy Reviews 15 (2011) 2921–2939

Contents lists available at ScienceDirect

Renewable and Sustainable Energy Reviews

journal homepage: www.elsevier.com/locate/rser

Convective heat transfer and fluid flow study over a step using nanofluids: A review

H.A. Mohammed[a,*], A.A. Al-aswadi[a], N.H. Shuaib[a], R. Saidur[b]

[a] Department of Mechanical Engineering, College of Engineering, Universiti Tenaga Nasional, Km 7, Jalan Kajang-Puchong, 43009 Kajang, Selangor, Malaysia
[b] Department of Mechanical Engineering, University of Malaya, 50603 Kuala Lumpur, Malaysia

ARTICLE INFO

Article history:
Received 11 August 2010
Accepted 4 February 2011

Keywords:
Backward facing step
Nanofluids
Nanoparticles
Heat transfer
Separation
Reattachment

ABSTRACT

Research in convective heat transfer on internal separated flows has been extensively conducted in the past decades. This review summarizes numerous researches on two topics. The first section focuses on studying the fluid flow and heat transfer behavior of different types of single-phase fluid flows over backward facing step (BFS) at different orientations. The second section concentrates on everything related to nanofluids; its preparation, properties, behavior, applications, and many others. The purpose of this article is to get a clear view and detailed summary of the influence of several parameters such as the geometrical specifications, boundary conditions, type of fluids, and inclination angle on the hydrodynamic and thermal characteristics using (BFS). The reattachment length and maximum Nusselt number are the main target of such research where correlation equations were developed and reported in experimental and numerical studies. The heat transfer enhancement of nanofluids along with the nanofluids preparation technique, types and shapes of nanoparticles, base fluids and additives, transport mechanisms, and stability of the suspension are also discussed.

Contents

* Corresponding author. Tel.: +60 38921 2265; fax: +60 38921 2116.
E-mail address: hussein@uniten.edu.my (H.A. Mohammed).

1364-0321/$ – see front matter
doi:10.1016/j.rser.2011.02.019

1. Introduction

The phenomena of flow separation and subsequent reattachment which occur due to a sudden expansion in the flow passages such as backward facing steps have been recognized as important industrial situations. This complex flow structure present in heating or cooling applications such as cooling electronic equipments, cooling turbines blades, combustion chambers, chemical processes, cooling of nuclear reactors, wide angle diffusers, high performance heat exchangers, energy systems equipment, and flow in valves. In many instances separation of flow is undesirable and leads to unwanted pressure drops and energy losses which require additional fan or pumping power to overcome them. However, in other circumstances flow separation may be encouraged, such as in burner flame stabilization use for turbulence promotion leading to enhanced mixing or heat and mass transfer rates.

The problem of flow over backward facing step has been extensively investigated, both experimentally and numerically. However, case studies such as injection flow, ribs geometry, double step ducts, and onset inlet flow, are not considered in the present review. The current review will only consider the studies of the case of steady-state convective flow and heat transfer over single backward facing steps.

A large number of experimental and numerical studies focus on flow and heat transfer behavior of convective flow over backward facing step geometry have been reported. These vast results and information have dealt with different conditions, parameters, geometry dimensions, and instrumentation, which indeed to undefined solid base for comparison purposes to indicate more accurate methodology for solving the case studies.

The dispersion of these results were attracted the attention of many researchers to unify the information to a general criteria. In 1992 and 1993, the Aerospace Heat Transfer Committee (K-12) of the Heat Transfer Division of the ASME held a technical session for benchmark heat transfer problems during the Winter Annual Meeting to solve numerically laminar mixed convection flow over two-dimensional horizontal and vertical backward facing step, respectively [1–3]. Moreover, due to the importance of the separation and reattachment phenomenon Abu-Mulaweh in 2003 [4] reviewed the results of flow and heat transfer of single-phase laminar mixed convection flow over different orientations of both backward and forward facing steps for several previous work. Most of the studies in this literature declared that only one large primary recirculation region develops downstream of the backward-facing step, while in some cases a secondary recirculation may develop between the downstream stepped wall and the step or at the top wall of the duct due to increase in step height and inlet velocity.

The purpose of this paper is threefold. The primary purpose is to review the available results of the flow and heat transfer presented in previously published data for single backward facing step. The results of massive number of different parameters affect the fluid flow and heat transfer characteristics are summarized and presented with a large number of correlation equations to predict the peaks of the flow and heat transfer in the recirculation regions. The second purpose is to understand the characteristics and functions of nanofluids, to expect their effects and heat transfer enhancement in such geometries. The third purpose is to open a gate for new researches and propose suggestions that could lead to improve the ability to predict separation and reattachment phenomenon

Nomenclature

AR	aspect ratio (W/s)
C_p	specific heat (kJ/kg K)
ER	expansion ratio (*H/h*)
f	elliptic relaxation function
Gr	Grashof number ($g\beta\Delta Ts^3/\nu^2$)
g	gravitational acceleration
H	total channel height (m)
h	inlet channel height (m)
k	thermal conductivity (W/m K)
k	turbulent kinetic energy (m^2/s^2)
L	total length of the channel (m)
Nu	local Nusselt number (hL/k)
Nu_{max}	local Nusselt number (hL/k)
P	pressure (Pa)
q	heat flux (W/m^2)
Re	Reynolds number ($\rho U_0 h/\mu$)
Ri	Richardson number
s	step height (m)
T	temperature (K)
U_0	bulk velocity at the inlet (m/s)
u	velocity component × direction (m/s)
v	velocity component *y* direction (m/s)
w	velocity component *z* direction (m/s)
$x_{u,w}$-lines	$[(du/dy)_{z=const}\|_{y=0}]$
x, *y*, *z*	Coordinate directions
X_i, X_e	upstream, downstream lengths (m)
X_r, X_0, X_n	peak points

Greek symbols

β	thermal expansion coefficient (1/*T*)
ρ	density (kg/m^3)
μ	dynamic viscosity (N m/s)
φ	nanoparticles volume fraction
Δ	amount of difference
ϕ	inclination angle
ν	kinematic viscosity (m^2/s)
ϖ	dimensionless oscillation frequency
ε	turbulent dissipation rate (m^2/s^3)
ξ	buoyancy parameter (Gr_s/Re_s^2)
ζ	v^{-2}/k

Subscripts

0	inlet
w	wall

using nanofluids. The review starts with an extensive review on the flow and heat transfer in backward facing step channels. After that, a comprehensive review for nanofluids and its characteristics is described. At the end, the review concentrates on the flow and heat transfer over a backward facing step using nanofluids.

2. Flow geometry

The general feature of backward facing step flow has the simplest reattachment flow, but the flow field is still very complex. The scope of this review is to summarize the previous efforts that studied the single-phase convective flow over two and three dimensional horizontal single backward facing step expansion in horizontal, inclined, and vertical orientations. A schematic diagram for backward facing step at either uniform wall temperature (UWT) or uniform heat flux (UHF) is shown in Fig. 1.

The advent of new instrumentation such as laser anemometer, pulsed-wire anemometer, laser-Doppler measurement, hot wire probes, etc., have made a renaissance for proliferation of new researches in this area and facilitate the study of sophisticated three-dimensional flow structures associated with separation and reattachment phenomena in this geometry. In experimental studies, the fluid velocity and temperature distributions were measured using Laser-Doppler velocitimeter and cold-wire anemometer, respectively, at any location. In numerical studies, the step geometry and its boundary conditions were modeled using Boussinesq approximation. The steady three-dimensional mass conservation, momentum equations, and energy equation governing the fluid flow and heat transfer problem are reduced to the following forms [5]:

Continuity equation:

$$\frac{\partial(\rho u)}{\partial x}+\frac{\partial(\rho v)}{\partial y}+\frac{\partial(\rho w)}{\partial z}=0$$

X-momentum equation:

$$\left(u\frac{\partial(\rho u)}{\partial x}+v\frac{\partial(\rho u)}{\partial y}+w\frac{\partial(\rho u)}{\partial z}\right)=-\frac{\partial P}{\partial x}\left[\frac{\partial}{\partial x}\left(\mu\frac{\partial u}{\partial x}\right)+\frac{\partial}{\partial y}\left(\mu\frac{\partial u}{\partial y}\right)+\frac{\partial}{\partial z}\left(\mu\frac{\partial u}{\partial z}\right)\right]$$

Y-momentum equation:

$$\left(u\frac{\partial(\rho v)}{\partial x}+\frac{\partial(\rho v)}{\partial y}+\frac{\partial(\rho v)}{\partial z}\right)=-\frac{\partial P}{\partial y}+\rho_0\beta(T-T_0)g_y=\left[\frac{\partial}{\partial x}\left(\mu\frac{\partial v}{\partial x}\right)+\frac{\partial}{\partial y}\left(\mu\frac{\partial v}{\partial y}\right)+\frac{\partial}{\partial z}\left(\mu\frac{\partial v}{\partial z}\right)\right]$$

Z-momentum equation:

$$\left(u\frac{\partial(\rho w)}{\partial x}+v\frac{\partial(\rho w)}{\partial y}+w\frac{\partial(\rho w)}{\partial z}\right)=-\frac{\partial P}{\partial z}\left[\frac{\partial}{\partial x}\left(\mu\frac{\partial w}{\partial x}\right)+\frac{\partial}{\partial y}\left(\mu\frac{\partial w}{\partial y}\right)+\frac{\partial}{\partial z}\left(\mu\frac{\partial w}{\partial z}\right)\right]$$

Energy equation:

$$\left(u\frac{\partial(_\rho C_pT)}{\partial x}+v\frac{\partial(_\rho C_pT)}{\partial y}+w\frac{\partial(_\rho C_pT)}{\partial z}\right)=\left[\frac{\partial}{\partial x}\left(\mathrm{k}\frac{\partial T}{\partial x}\right)+\frac{\partial}{\partial y}\left(\mathrm{k}\frac{\partial T}{\partial y}\right)+\frac{\partial}{\partial z}\left(\mathrm{k}\frac{\partial T}{\partial z}\right)\right]$$

There are different techniques were used to solve the partial differential equations along with specific boundary conditions, such as finite difference (FD), finite volume (FV), finite element (FE), or lattice Boltzmann (LB). These methods are solved by using different numerical software codes such as FLOTRAN, FLUENT, TEACH, COUGAR, KAMELEONII, FIDAP, NEKTON, CUTEFLOWS, QMRCGS, etc.

3. Backward facing step geometry

Convective flow and heat transfer over a backward facing step has been extensively investigated in the last decades, both experimentally and numerically. It has been reported in the literature that the first effort for studying the separation and reattachment flow over a backward-facing step was done in the late 1950s. The advent of new instrumentation and the improvement of the numerical codes increase the number of new researches in such problem and facilitate the complex study of three-dimensional flow in the separation and reattachment zone. The horizontal, inclined, vertical cases were investigated for different geometrical, boundary conditions and fluids properties.

3.1. Horizontal flow

One of the first investigations dealt with laminar regime and subsonic free stream flowing over a step was presented by Goldstein et al. [6]. They concluded, based on their experimental measurements, that in laminar regime the reattachment point is not a constant value as in turbulent regime, but it depends on the boundary displacement thickness and the hydraulic Reynolds number. Interest in studying the reattachment phenomena over the backward-facing step continued in the 1970s and 1980s. Experimental and numerical studies for 2D pure forced convection flow where there is no heat transfer effect have been investigated by Denham and Patrick [7], and Armaly et al. [8,9].

Denham and Patrick [7] studied the measurements of 2D laminar flow over backward-facing step. The water flow in a range of Reynolds number ($50 \le Re \le 250$) passed through a single plane duct expansion with an expansion ratio and aspect ratio of ER = 3, and AR ≈ 20, respectively. They indicated that the general flow field bears similarities to other recirculating flows like axi-symmetric and the 2D duct sudden expansions but recirculation zone lengths and recirculated mass flow rates were smaller at a given value of Reynolds number. They noticed that a small fluctuation occurs at $Re = 229$ while the other lower values remain steady; this fluctuation observed to be the onset of transition to turbulence of the separated boundary layers. Furthermore, it was found that there is a tendency towards secondary separation at the upper wall as reattachment occurs, this phenomenon was produced due to the inflections of the velocity profiles and it was clearer at the highest Reynolds number.

The effect of Reynolds number for different flow regimes was conducted by Armaly et al. [8]. They reported the measurements of velocity distribution and reattachment length through downstream of a single backward-facing step mounted in a two-dimensional channel. Air was used as a working medium with Reynolds number range of $70 < Re < 8000$ in a test section has a high aspect ratio of AR = 36. Numerical predictions were also presented to be compared with the experimental results as the flow maintained its two-dimensionality in the experiments. The comparison showed a good agreement with the experimental findings

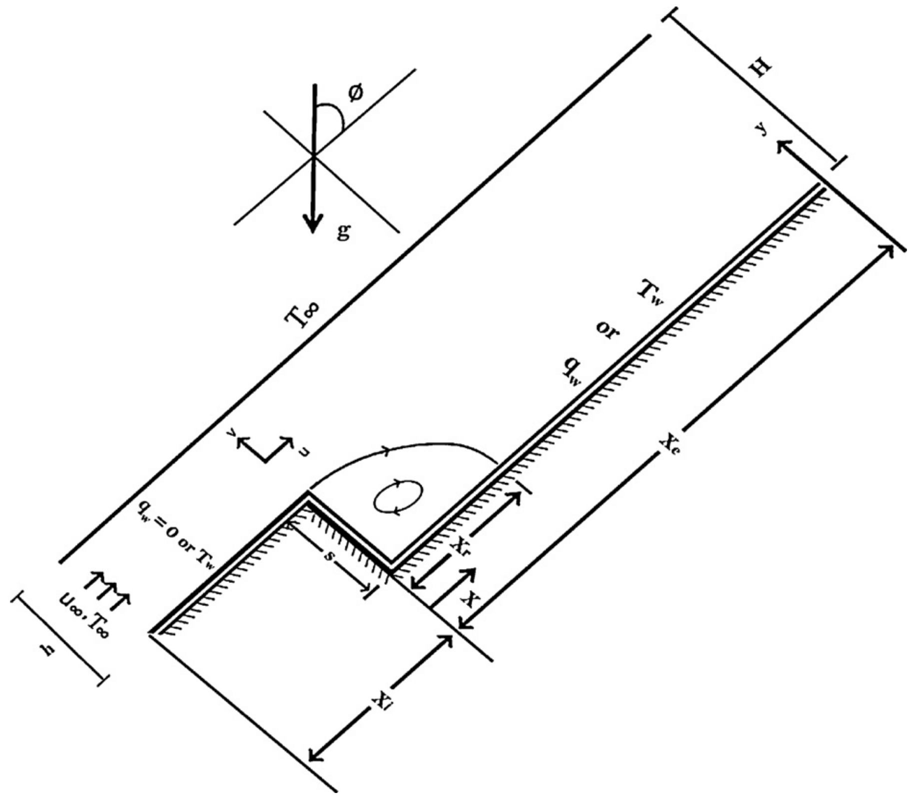


Fig. 1. Schematic diagrams for backward-facing step.

up to a Reynolds number $Re \approx 400$. Armaly et al. [9] showed that the vortices start to develop in the laminar region at $Re \approx 800$, but it becomes very pronounced at $Re = 2300$, and damped out at $Re = 5000$. It was indicated that in both the pure laminar ($Re \lesssim 400$) and the fully turbulent ($Re \gtrsim 6600$) flow regimes, the flow is indeed two-dimensional over large parts of the width of the test section.

Most of the existing research efforts have been focused on two-dimensional situations, though most of the realistic applications are practically dominated by three dimensional geometries. In the early 1990s many researchers tend to study the flow field in three-dimensional due to the presence of certain effects which are not visualized in two-dimensional (at centerline of the plane) such as the side-wall effect. The three-dimensional pure forced convection flow have been extensively investigated by Shih and Ho [10], Chiang et al. [11], De Brederode and Bradshaw [12], Hertzberg and Ho [13], Tylli et al. [14], Armaly et al. [15], and Nie and Armaly [16]. Shih and Ho [10] examined the water flow field behind a small aspect ratio backward-facing step with AR = 3 using Laser-Doppler Anemometer. The measurements of the three velocity components inside the separation region indicated that the flow is highly three-dimensional. The mean reattachment line is highly distorted across the span with the shortest reattachment position located at the centreline and about 20% shorter than the value closer to the side wall. The maximum spanwise velocity component was indicated to be of the same order as the streamwise velocity at the point near the center of the step.

Chiang et al. [11] aimed to clarify and present a deep explanation on skin-friction fields as a guide for exploring the physical interpretation of the three-dimensional flow separation behind the step, reattachment of the flow, and the roof recirculatory flow pattern. The channel designed to have an expansion ratio ER = 1.9432 where the step was 0.9432. The parametric study was carried out by varying Reynolds numbers and various spans with values not greater than 800 and 10, respectively. It was shown that the flow separation-attachment occurs on the roof of the channel but it confined only to the sidewall region. The roof recirculation zone size is dependent on Reynolds number.

The distance between the side-walls plays a significant effect with aspect ratio of the backward-facing step ducts. De Brederode and Bradshaw [12] systematically studied the side wall effects with top hat free stream velocity profile. It was concluded that the three-dimensional features could be neglected if the aspect ratio of the step was larger than 10. Furthermore, Hertzberg and Ho [13] observed that the presence of the strong spanwise velocity in a small aspect ratio rectangular sudden expansion will obviate the formation of the recirculation zone after the step and therefore has a zero reattachment length.

Tylli et al. [14] studied the sidewall effects in three-dimensional laminar water flow over a backward-facing step experimentally and numerically. Experiments were based on both digital and stereoscopic particle image velocimetry; a spectral element method was used for the laminar, transition, and turbulent simulations. The geometry has an expansion ratio, ER, and aspect ratio, AR, of 2 and 20, respectively. It was noticed that excellent agreement between the 3D simulation and the experiments is obtained when Reynolds number reaches $Re \approx 650$. Moreover, it was found that at low Reynolds numbers ($Re < 400$), side wall effects do not affect the structure of laminar flow in the channel mid plane; thus, the mid plane field is accurately predicted by two-dimensional simulations. In addition, it was found that at higher Reynolds numbers, laminar flow is characterized by sidewall separation and the formation of a recirculation zone, which, however, does not penetrate up to the channel mid plane. The wall-jet intensity and flow three-dimensionality increase with Reynolds number for laminar flow, and decrease for transitional flow; three-dimensional variation is hardly noticed in the time average field of turbulent flow.

Armaly et al. [15] measured the velocity for three-dimensional laminar separated airflow adjacent to a backward-facing step using two-component laser Doppler velocimeter. The backward-facing step, with a height of $s = 1.0$ cm has an aspect ratio of AR = 8, and an expansion ratio of ER = 2.02. The flow measurements were covered Reynolds number range between $98.5 \le Re \le 525$ to develop a clear view of both sidewall and the step effects, and compared with the previous 2D studies. It was determined that for $Re \le 98.5$ there was no recirculation flow region adjacent to the sidewall and at $Re \le 190$, a small recirculation flow region was detected in the upper corner of the sidewall. It was concluded that the spanwise and the transverse peak velocities move to the center of the duct as the distance from the step increases.

Nie and Armaly [16] measured the velocity adjacent to the bounding walls of three-dimensional backward-facing step flow using Laser-Doppler velocimeter. The study was performed for the purpose of mapping the boundaries of the reverse flow regions that develop adjacent to the walls of a geometry with a step height $s = 1$ cm, aspect ratio AR = 8, and an expansion ratio ER = 2.02 as a function of Reynolds number. The Reynolds numbers were presented in the range of $100 \le Re \le 8000$ to cover the three types of flow regimes. The boundaries of the reverse flow regions were identified by locating the streamwise coordinates on a plane adjacent to the bounding walls where the mean streamwise velocity component is zero. The three-dimensional reattachment point at the stepped wall was compared with the two-dimensional at the center of the test section. It was noticed that the three-dimension flow results are slightly higher in the laminar flow regime ($Re < 400$); significantly lower in the transition flow regime ($400 < Re < 3400$); and slightly lower in the fully turbulent flow regime as ($Re > 3400$). It was noticed that the size of the reverse flow regions increases and moves further downstream in the laminar flow regime; decreases and moves upstream in the transitional flow regime; and remains almost constant or diminishes in the turbulent flow regime; as the Reynolds number increases.

The literature review reveals that there were several studies focused on the heat transfer phenomena over the backward-facing step which exhibit an influence in the fluids flow behavior. Aung [17], and Sparrow and Chuck [18] are the first investigators who established and reported an experimental and numerical results on heat transfer for 2D laminar air flow passing a backward-facing step channel heating at uniform temperature from below. In their studies, they outlined that for laminar airflow the heat transfer increases monotonically in the stream-wise direction and quantitatively it is less than that of the flat plate value. It was concluded that the Nusselt number was independent of the Reynolds number; the local Nusselt number distribution begins with a low value at the step, and then increases monotonically and attains a maximum value at a position near the reattachment point then it decreases monotonically towards the fully developed value.

Khanafer et al. [19] analyzed mixed convection of laminar pulsatile flow and heat transfer past a backward-facing step in a channel. Fluid flow and heat transfer characteristics were examined in the domain of the Reynolds number, Richardson number and the dimensionless oscillation frequency as: $100 \le Re \le 1000$, $1.78 \times 10^{-3} \le Ri \le 10$, and $0.1 \le \varpi \le 5$. It was found that the elimination of the separation region occurs for $Ri > 0.1$, and as Reynolds number increases, the recirculation zone along the heated downstream surface becomes larger. The thermal boundary layer decreases in thickness as Reynolds number increases and consequently increases the heat transfer rate. The average Nusselt number and the length of the recirculation zone decrease with an increase in Richardson number. It was also noticed that the dimensionless local variation of skin friction coefficient along the heated wall increases with increasing the Richardson number.

Chen et al. [20] simulated numerically the turbulent forced convective flow adjacent to a two-dimensional backward-facing step. The objective of this study was to explore the effects of step height on turbulent separated flow and heat transfer. The stepped wall downstream from the step was set to be uniform and constant heat flux $q_w = 270\,W/m^2$, while other walls were treated as adiabatic. Reynolds number and duct's height downstream from the step were kept constant at $Re_0 = 28{,}000$ and $H = 0.19$ m, respectively. On the other hand, the expansion ratio was maintained to ER = 1.11, 1.25, and 1.67, respectively. It was noticed that as the step height increases; the primary and secondary recirculation regions, magnitude of the maximum turbulent kinetic energy increase, and the bulk temperature increases rapidly as well. Near the step and below the step height, it was found that the kinetic energy becomes smaller as the step height increases. Moreover, it was found that the maximum temperature becomes greater as the step height increases. The peak values of the transverse velocity component become smaller as the step height increases, but inside the recirculation region; the skin friction coefficient becomes less significant and smaller in magnitude with the increase of the step height.

The effects of the flow and heat transfer in a 3D backward-facing step ducts have been extensively studied using different parameters by Iwai et al. [21], Nie and Armaly [22], Armaly et al. [23], Barbosa Saldana and Anand [24], Barbosa Saldana et al. [5], and Lan et al. [25]. Iwai et al. [21] performed a numerical simulation for three-dimensional mixed convection flows over a backward-facing step at low Reynolds number in order to investigate the effects of the duct aspect ratio. Numerical results were conducted for an aspect ratio range between $4 \le AR \le 24$, and Reynolds number range between $125 \le Re \le 375$ to study its effects on Nusselt number and the skin friction coefficient on the bottom wall. It was found that an aspect ratio of 16 at least is needed to secure 2D region in the central part of the duct at a Reynolds number of 250. It was also found that the maximum Nusselt number increases with an increase of the aspect ratio and Reynolds number. The skin friction coefficient is found to be an analogous to the case of Nusselt number distribution.

Nie and Armaly [22] presented a numerical analysis for a three-dimensional incompressible laminar forced convection flow adjacent to backward-facing step in rectangular duct. The effects of step height on the flow and heat transfer characteristics were the main objectives of this study. The geometry, thermophysical properties, and flow condition are based on the available measurements of Armaly et al. [23]. The simulations were performed at $Re = 343$ for different step heights ($s = 0.008$, 0.010, and 0.012 m), while the other geometries were kept constant. It was found that increasing the step height increases the reattachment length, the Nusselt number, the size of the sidewall reverse flow region, and the general three-dimensional features of the flow. In addition, as the step height increases, the distance between the step and the point where the impingement flow reaches the stepped wall downstream increases, and a secondary recirculation flow region develops adjacent to the bottom corner of the step. For the case of small step height ($s = 0.008$ m), the minimum Nusselt number is located near the bottom corner between the step and the centerline of the duct. As the step height increases, the minimum Nusselt number is appeared to move towards near the bottom corner of the step and the sidewall. It was found that the friction coefficient increases in the streamwise direction along the centerline of the duct inside the primary recirculation flow region, but it decreases outside the recirculation region with increasing step height.

Barbosa Saldana and Anand [24] studied numerically forced convective airflow over a three-dimensional backward-facing step. The horizontal backward-facing step channel was set to have a step height $s = 1$ cm, an aspect ratio of 8 and an expansion ratio of 2. The

stepped wall was fixed to a constant heat flux $q_w = 50\,W/m^2$ while the other walls were considered as insulated. The Reynolds numbers were set to be in the range of 98.5 and 512. The local Nusselt number along the bottom wall was found to lie in the vicinity of the x_u-line and the x_w-line points of intersection where the shear stress along the bottom wall is equal to zero. Furthermore, the velocity profiles revealed that for Reynolds number greater than 343 the flow does not reach fully developed conditions at the channel exit.

Barbosa Saldana et al. [5] simulated numerically laminar mixed convective flow over a three-dimensional horizontal backward-facing step. All the walls are treated adiabatically except the bottom wall of the channel is subjected to a constant high temperature. An airflow of fixed Reynolds number $Re = 200$ enters hydrodynamically fully developed and isothermally in a duct with an aspect ratio of 4, expansion ratio of 2, and total length of 52 times the step height $L = 52S$. It was reported that as Richardson number (Ri) increases; the location of x_u-line displaces to the upstream (higher velocity components), the recirculation zone is shortened, vertical size of the recirculation zone reduced, and negative values of u velocity (streamwise direction) next to the bottom wall of the channel increases. In addition, as the Richardson number increased; the location of the maximum averaged Nusselt number distribution was moved and the maximum averaged streamwise shear stress distribution moved its location further upstream.

Lan et al. [25] simulated the turbulent forced convection adjacent to three-dimensional backward-facing step in a rectangular duct using a ($k-\varepsilon-\zeta-f$) turbulent model. The aim of the study was to present a clear, realistic, and more accurate investigation near the walls to predict the turbulent heat transfer separated and wall-bounded flows better than the commonly used two-equation turbulence model. A User Defined Function (UDF) was implemented using FLUENT-CFD, and two-dimensional benchmark problems were simulated to validate the three-dimensional simulation code. The geometry has an expansion ratio and a step height of 1.48 and 4.8 mm, respectively. The three aspect ratios of 3, 8 and infinity (2-D simulation) were considered for studying its effect on the flow and heat transfer. The effect of Reynolds number in the range of $20{,}000 \le Re \le 50{,}000$ was also considered. The effects of the Reynolds number and aspect ratio on the flow reattachment was minimal in the range of parameters that were examined, but they were shown to have significant influence on the heat transfer. The reattachment length was found to be constant in central portion of duct width, but starts to increase as it approaches the side walls and reaches its maximum value on the side walls. It was noticed in the primary recirculation flow region and in the vicinity of the recirculation line a significant spanwise flow developed. The maximum local Nusselt number was found to be developed in the region where the spanwise velocity is maximum adjacent to the heated wall close to the sidewall. The bulk air temperature was found to decrease as the Reynolds number increases, but it was not influenced significantly by the changes in the aspect ratio.

3.2. Inclined flow

The backward-facing step channel orientation effects attracted some researchers such as Lin et al. [26], Lin et al. [27], Hong et al. [28], Abu-Mulaweh et al. [29], and Iwai et al. [30] to investigate the separation region and the reattachment point with respect to other parameters. The literature declared that the first effort dealt with backward-facing step in inclined duct was introduced by Lin et al. [26]. They examined numerically the effects of inclination angle ($0^\circ \le \phi \le 90^\circ$ from the vertical) on the two-dimensional mixed convective laminar flow and heat transfer in a duct with a backward-facing step under buoyancy-assisting flow conditions. The case study was taken from a previous study done by the same author for a vertical duct with a backward-facing step Lin et al. [27]. The geometry has an expansion ratio and step height, of 2 and 0.48 cm, respectively. The straight wall at the top of the duct was maintained at the inlet air temperature of 20 °C, the downstream stepped wall was maintained to a uniform temperature of 35 °C, while the upstream wall and the step were maintained adiabatic. The Reynolds number was maintained at 50. It was found that the recirculation size increases as the orientation transfer from the vertical axis. The streamwise component of the Grashof number has a strong influence on the flow, but the transverse component has a small effect on the velocity and temperature profiles in the fully developed regime. The substantial fact elaborates that the reattachment length, fluid temperature, and the shear stress at the unheated wall increase as the inclination angle increases from the vertical. In contrary, for Nusselt number for both heated and unheated walls, the streamwise buoyancy force, and the shear stress at the heated wall are decreased.

Hong et al. [28] were the first who investigated the buoyancy opposing effects in an inclined channel with a backward-facing step. They studied numerically the influence of the relevant inclination angle and Prandtl number for two-dimensional laminar mixed convective airflow for buoyancy assisting and opposing flow conditions. The geometry has an expansion ratio and step height, of 2 and 0.0048 m, respectively. The straight wall at the top of the duct was maintained at the inlet air temperature of 293 K, the downstream stepped wall was maintained to a uniform heat flux of $200\,W/m^2$, while the upstream wall and the step were maintained adiabatic. The Reynolds number was fixed at 100, and the Grashof number was fixed at 609. The inclination angle was varied from 0° to 360°, while other parameters were kept constant. It was found that as the inclination angle increases from 0° to 180°, the reattachment length increases, but the wall friction coefficient and the Nusselt number at the heated wall decrease. Moreover, the transverse buoyancy force was noticed to have a less significant effect on the flow and heat transfer downstream the reattachment point, while it has a strong effect in the recirculation region. The Prandtl number was varied in the range of $0.07 \le Pr \le 100$, while the inclination angle was fixed at 0°. It was found that as the Prandtl number increases, the Nusselt number and the reattachment length increase, but the wall friction coefficient decreases.

The understanding of the separated zone and reattachment process was poor for the inclined channel with a backward-facing step due to the inability to predict simple reattaching flows over a wide range of parameters. The first experimental effort dealt with backward-facing step mounted in inclined channels is presented by Abu-Mulaweh et al. [29]. They measured experimentally and simulated numerically the influence of buoyancy-assisting laminar mixed convection in boundary-layer flow over horizontal and inclined two-dimensional backward-facing step. The objectives of the study were to determine the reattachment length and the onset of vortex instability for different wall temperatures ($0 \le \Delta T \le 30\,°C$), free stream velocities ($0.285 \le u_\infty \le 0.7$ m/s), step heights ($0.35 \le s \le 0.8$ cm), and inclination angles ($30^\circ \le \phi \le 90^\circ$) as measured from the vertical direction. The geometry of the test section was consisted of a heated constant temperature downstream section, adiabatic upstream section and step, and the top section was a free stream. It was noticed in horizontal case that the buoyancy force has a negligible effect on the velocity and temperature distributions, but it significantly influences the onset of instability. On the other hand, it was found that as the inclination angle increases from the vertical, the streamwise component of the buoyancy force decreases, which causes an increase in the velocity gradient and a decrease in the temperature gradient at the wall in the recirculation region. It was concluded that as the inclination angle increases from the vertical, the local Nusselt number decreases, while the reattachment length and the

location of the maximum Nusselt number behind the backward-facing step increase. It was noticed that the maximum Nusselt number occurs downstream of the reattachment point. Moreover, the space between the maximum Nusselt number location and the reattachment decreases slowly as the inclination angle increases.

As it has been introduced in the previous sections, all of the existing researches for the inclined channel with a backward-facing step are focused on two-dimensional situations, though most of the realistic applications are practically dominated by three dimensional geometries. It is declared from the literature that the first three-dimensional study is presented by Iwai et al. [30]. They simulated numerically the effect of inclination angle in three-dimensional mixed convective flow over a backward-facing step in a rectangular duct. The downstream wall was kept with a constant heat flux, while other walls were kept adiabatic. Parameters such as Reynolds number, expansion ratio, and aspect ratio were kept constant, at 125, 2, and 16, respectively. The effects of two inclination angles; ϕ_1 pitch angle changing in the range of $0^\circ \le \phi_1 \le 360^\circ$, and ϕ_2 rolling angle changing in the range of $0^\circ \le \phi_2 \le 180^\circ$ are the main interest of this study. The three positions of the reattachment point X_r, the peak Nusselt number point X_p and the downstream end of the secondary recirculation region X_s on the centerline of the heated wall are shifted with ϕ_1. It was found that when ϕ_1 is changed while keeping ϕ_2 to be zero degree, positions of the maximum Nusselt numbers are symmetrically obtained at the positions on the heated wall near the two side walls, similar to the cases of pure forced convection. The maximum Nusselt number was appeared at the most upstream position in the case of $\phi_1 = 0^\circ$, and the minimum at the most downstream position in the case of $\phi_1 = 180^\circ$. On the other hand, it was noticed that when ϕ_2 is changed while keeping ϕ_1 to be 90°, the flow and thermal fields become asymmetric about the duct centerline. It was observed that ϕ_2 has little effect on the spanwise position of the maximum Nusselt number.

3.3. Vertical flow

It is indicated from the literature that the first effort of studying the effects of vertical backward-facing step was introduced by Lin et al. [31]. They examined and reported the numerical results of laminar mixed convection airflow and heat transfer, buoyancy-assisting through a two-dimensional vertical duct with a backward-facing step. The study was conducted to cover the domain from pure forced convective flow to the inlet starved convective flow where the average inlet velocity is smaller than the corresponding natural convective value. The geometry dimensions and boundary conditions were based on previous work done by Armaly et al. [7]. The influence of the temperature difference between the heated wall downstream of the step and free stream in the range of $1 \le \Delta T \le 75\,^\circ$C was detected. It was found that as the wall temperature increases, the reattachment length decreases and the size of the secondary, inner recirculation region that develops at the corner between the heated wall and the step increases. On the other hand, the buoyancy level decreases for a fixed wall temperature as the Reynolds number increases. It was noticed that the force of the pressure drop F_p is lower than the force of the kinetic energy F_k, where a reverse flow could be developed from the downstream section of the duct along the cooler wall as outlined by Aung and Worku [32]. However, it was found that the disappearance of the reattachment from the heated wall will occur only in the starved flow regime. The Nusselt number was found to be increased as the wall temperature increases and the Reynolds number decreases. Both the peak Nusselt number length X_n, and the reattachment length of the main recirculation region, X_r, decrease, while the length of the recirculation region, X_o, increases as the value of the buoyancy parameter increases. Moreover, the peak Nusselt number occurs downstream of the reattachment point and the spacing increases as the buoyancy parameter increases.

The effects of step height in inclined ducts that presented before in this literature did not include the vertical orientation ($\phi = 0^\circ$). This gap of research motivated Hong et al. [4,33] to investigate the effects of other parameters due to different step height. They numerically studied the effects of the mixed convection flow and heat transfer through a two-dimensional vertical duct having a backward-facing step. The downstream wall from the step was subjected to a uniform heat flux (UHF), while the upstream wall and the step by itself were adiabatic, and the straight top wall was maintained at a uniform temperature that is equal to the inlet fluid temperature. Furthermore, they examined the effects of different ranges of parameters such as Grashof number, $0 \le Gr_s^* \le 24{,}000$, expansion ratio, $1.25 \le ER \le 4$, and Reynolds number, $0 \le Re \le 150$. It was found that Grashof number has a significant influence on the flow and heat transfer; when Grashof number increases, the wall friction coefficient and the local Nusselt number on the downstream heated wall increase, and verse visa for the reattachment length. It was noticed that the reattachment length increases as the expansion ratio increases for less than 2.25, but for values greater than 2.25 the reattachment length decreases. Moreover, it was found that increasing the expansion ratio increases the fully developed value of the wall friction coefficient and the distance for the flow to reach the fully developed regime, but it decreases the peak and the fully developed Nusselt numbers. They have developed correlation equations for reattachment length and the peak Nusselt number as shown in Table 1.

Baek et al. [34] studied experimentally and numerically the buoyancy-assisting laminar mixed convection airflow and heat transfer over a vertical, two-dimensional backward-facing step. Different free-stream velocities, wall temperature differences, and step heights in the range of ($0.37 \le u_o \le 0.72$ m/s), ($10 \le \Delta T \le 30\,^\circ$C), and ($0.38 \le s \le 1$ cm), respectively, were considered to visualize the flow and heat transfer behavior. It was found that for a fixed inlet velocity, the reattachment length, X_r, decreases as the wall temperature increases. Similarly, for a fixed wall temperature, the reattachment length, X_r, and the volume of the recirculation region decrease as the inlet velocity decreases. It was noticed that the recirculation region disappears and detaches from the heated wall and attaches only to the adiabatic step. Moreover, for the heat transfer visualization, it was found that the heat transfer rate is seen to increase as the temperature difference increases. The fluid temperature in the recirculation region behind the step ($X < X_r$) was considerably higher than the temperature downstream of the reattachment point ($X > X_r$). As the buoyancy force increases, the magnitude of the Nusselt number increases and the location of its peak moves closer to the step. An effort was made by the authors to modify the existing empirical correlation for the reattachment length in the laminar forced convection flow, as given by Goldstein et al. [6], to reflect also the influence of step height and buoyancy parameter. It was found that the location of the maximum Nusselt number, X_n, and the reattachment length, X_r, decreases as the buoyancy force increases.

Abu-Mulaweh et al. [4,35] examined the influence of buoyancy-assisting laminar flow and heat transfer over a 2D vertical backward-facing step. The boundary conditions and general step geometry were taken from Baek et al. [34] except the downstream heated wall was maintained to a uniform heat flux in the range between $102 \le q_w \le 290$ W/m^2. As the buoyancy force increases, the reattachment length X_r decreases but the local Nusselt number increases and the location of its maximum values moves closer to the step. Moreover, it was found that the local Nusselt number to be lower in the region where $X < X_r$ and higher in the region where $X > X_r$ for higher free stream velocity. Correlation equations for the reattachment length were reported in Table 1.

Table 1
Summary of the research done on backward facing step.

	Orientation	Heating type	Fluid	Dim study	Study	Ranges	X_r correlation equations	X_0 correlation equations	X_n correlationequations	$Nu_{s,max}$ correlation equations
Denham and Patrick [7]	Hor	–	Water	2D	E	$50 \le Re \le 250$ ER = 3 AR ≈ 20	–	–	–	–
Armaly et al. [8]	Hor	–	Air	2D	E & N	$70 \le Re \le 8000$ ER = 1.9423 AR = 36	–	–	–	–
Shih and Ho [10]	Hor	–	Water	2D&3D	E	AR = 3 Laminar	–	–	–	–
Chiang et al. [11]	Hor	–	Oil	3D	E	$Re \le 800$ ER = 1.9432 AR = 10.6022	–	–	–	–
Tylli et al. [14]	Hor	–	Water	3D	E & N	Lam $\le Re \le$ Tur ER = 2 AR = 20	–	–	–	–
Armaly et al. [15]	Hor	–	Air	3D	E & N	$98.5 \le Re \le 525$ ER = 2.02 AR = 8	–	–	–	–
Nie and Armaly [16]	Hor	–	Air	3D	E	$100 \le Re \le 8000$ ER = 2.02 AR = 8	–	–	–	–
Khanafer et al. [19]	Hor	UWT[a]	Air	2D	N[a]	$100 \le Re \le 1000$ $1.78E^{-3} \le Ri \le 10$ $0.1 \le \varpi \le 0.5$ AR = 8	–	–	–	–
Chen et al. [20]	Hor	UHF[a]	Air	2D	N	$Re = 28000$ $1.11 \le ER \le 1.67$	–	–	–	–
Abu-Nada [169]	Hor	UWT	NF[a]	2D	N	$200 \le Re \le 600$ $0 \le \varpi \le 0.2$ ER = 2	–	–	–	–
Iwai et al. [21]	Hor	UWT	Air	3D	N	$125 \le Re \le 375$ 4 $\le$ AR ≤ 24	–	–	–	–
Nie and Armaly [22]	Hor	UHF	Air	3D	N	$Re = 343$ $8 \le s \le 12$ mm	–	–	–	–
Saldana and Anand [24]	Hor	UHF	Air	3D	N	$98.5 \le Re \le 512$ ER = 2 AR = 8	–	–	–	–
Saldana et al. [5]	Hor	UWT	Air	3D	N	$Re = 200$ ER = 2 AR = 4	–	–	–	–
Lan et al. [25]	Hor	UHF	Air	3D	N	$2E^4 \le Re \le 5E^4$ ER = 1.48 $3 \le AR \le \infty$	–	–	–	–
Lin et al. [26]	Inc[a]	UWT	Air	2D	N	$0^\circ \le \phi \le 90^\circ$ $Re = 50$ ER = 2	–	–	–	–
Hong et al. [28]	Inc	UHF	Air	2D	N	$0^\circ \le \phi \le 360^\circ$ $0.07 \le Pr \le 100$ $Re = 100$ $Gr_s^* = 609$ ER = 2	$X_r = [5.462 - 1.62\cos(\phi)] \times [0.95 + 0.05\cos(2\phi)][1 + 0.02\sin(\phi)]$ $X_r = 4.9 - 1.7\exp(-Pr/0.4)$	$X_0 = \mathrm{MAX}\{0.4462\cos(\phi)[1 - 0.5\sin(\phi)],0\}$ $X_0 = 0.336 - 0.00165Pr$	$X_n = [5.472 - 0.6535\cos(\phi)][098 + 0.02\cos(2\phi)][1 + 0.02\sin(\phi)]$ $X_n = 3.53 + 1.71Pr$, $0.07 \le Pr \le 0.712$ $X_n = 4.753 - 0.0091Pr^2$, $0.712 \le Pr \le 100$	$Nu_{s,max}=[1.01 - 0.01\cos(2\phi)][1.752 + 0.151\cos(\phi)]$ $Nu_{s,max} = [0.52 + 1.29\sqrt{Pr}$

Abu-Mulaweh et al. [29]	Inc	UWT	Air	2D	E & N	$30^\circ \le \phi \le 90^\circ$ $50 \le Re_s \le 300$ $3.5 \le s \le 8$ mm $0 \le \Delta T \le 30\,^\circ C$	$X_r = 0.023(\delta_s/s)$ $Re_s + f(s/x_i) = 0.023$ $[5(x_i/s)Re_{xi}^{-1/2}]Re_s + f(s/x_i)$ $f(s/x_i) = 8995.8\,(s/x_i)^2 - 114.2$ $(s/x_i) - 3.4$	–	–	–
Iwai et al. [30]	Inc	UHF	Air	3D	N	$0^\circ \le \phi_1 \le 360^\circ$ $0^\circ \le \phi_2 \le 180^\circ$ $Re = 125$ ER = 2, AR = 16 $Ri = 0.03$	–	–	–	–
Lin et al. [31]	Ver[a]	UWT	Air	2D	N	$\phi = 0^\circ$ $Re_s = 50, 100$ $1 \le \Delta T \le 75\,^\circ C$ ER = 2	–	–	–	–
Hong et al. [33]	Ver	UHF	Air	2D	N	$\phi = 0^\circ$ $0 \le Re_s \le 150$ $0 \le Gr_s^* \le 2400$ $1.25 \le ER \le 4$	$X_r = X_{r,forced}\{1 + (7.188 - 4.047R$ $- 1.758Re_s)\xi\}$ $X_{r,forced} = a_0(R) + a_1(R)Re_s$ $a_0(R) = -1.252 + 1.345R - 0.1681R^2$ $a_1(R) = -0.02751$ $0.04572R - 0.006414R^2$	–	–	$Nu_{s,max} = 1.658 + 0.0001483Gr_s^*$ $Nu_{s,max} = 4.862 - 2.172R$ $+ 0.3292R^2$
Baek et al. [34]	Ver	UWT	Air	2D	E & N	$\phi = 0^\circ$ $0.37 \le u_\infty \le 0.72$ $10 \le \Delta T \le 30\,^\circ C$ $3.8 \le s \le 10$ mm	$X_r = (2.24 + 0.022Re_s)$ $\exp[-42\,\xi(s/x_i)^{-0.186}]$	–	–	–
Abu-Mulaweh et al. [35]	Ver	UHF	Air	2D	E	$\phi = 0^\circ$ $50 \le Re_s \le 330$ $0 \le \xi \le 1.4E^{-2}$ $3.5 \le s \le 8$ mm	$X_r = X_{r,forced}\,\exp(-7.5\,\xi^{1/2})$ $X_{r,force} = 0.023(\delta_s/s)Re_s + f(s/x_i)$ $f(s/x_i) = 8995.8\,f(s/x_i)^2 - 114.2$ $(s/x_i) - 3.4$	#	#	#
Abu-Mulaweh et al. [36]	Ver	UWT	Air	2D	E & N	$\phi = 180^\circ$ $0.41 \le u_\infty \le 0.66$ $0 \le \Delta T \le 30\,^\circ C$ $4 \le s \le 8$ mm	–	–	–	–
Iwai et al. [38]	Ver	UHF	Air	3D	N	$\phi = 0$ $0 \le \xi \le 0.12$ $Re = 125$ ER = 2, AR = 16	–	–	–	–
Abu-Mulaweh et al. [39]	Ver	UWT	Air	2D	E	$\phi = 0$ $0 \le u_\infty \le 0.41$ $S = 22$ mm	–	–	–	–
Abu-Mulaweh et al. [40]	Ver	UWT	Air	3D	E	$\phi = 0$ $u_\infty = 0.41$ m/s $0 \le s \le 22$ mm	–	–	–	–

[a] Hor, horizontal; Inc, Inclined; Ver, vertical; UHF, uniform heat flux; UWT, uniform wall temperature; NF, nanofluids; E, experimental; N, numerical; #, not identified; –, no correlation equation.

As introduced in the previous section in this literature, the researchers were concentrated on buoyancy-assisting vertical flow. The first effort to study the influence of the buoyancy-opposing flow was conducted by Abu-Mulaweh et al. [36]. They performed experimental and numerical studies of laminar flow over a vertical backward-facing step to measure the effect of the buoyancy-opposing on the airflow and heat transfer behavior. The experimental setup, test section and backward-facing step geometry, and the boundary conditions, are identical to that used by Abu-Mulaweh et al. [35] except that the orientation of the air tunnel is changed by 180° to create buoyancy-opposing flow conditions. It was noticed for low buoyancy levels $Ri < 4.4 \times 10^{-3}$; the length of the recirculation region downstream of the backward-facing step increases rapidly as the buoyancy level increases. However, for low buoyancy levels above 4.4×10^{-3}; the flow inside the recirculation region remains laminar but the length of the recirculation region decreases rapidly due to the effect of the transition of the flow from laminar to turbulent and the flow becomes turbulent downstream of the recirculation region. The effect of temperature difference between the heated wall downstream the step and the free stream in the range of $0 \leq \Delta T \leq 30\,^{\circ}\mathrm{C}$ was studied. It was found that as the temperature difference ΔT increases, the reattachment length increases and the Nusselt number decreases.

Abu-Mulaweh et al. [4,37] studied the effects of heating the upstream wall and the step of two-dimensional, vertical backward-facing step geometry on the flow and heat transfer characteristics in the region downstream of the step. Four different upstream wall and step heating conditions were examined. The first case Temperature Boundary Condition (TBC) was TBC-1, which corresponds to $T_{w1} - T_{\infty} = T_w - T_{\infty}$, the second case was TBC-2 corresponds to $T_{w1} - T_{\infty} = 2(T_w - T_{\infty})$, the third case was TBC-1/2 corresponds to $T_{w1} - T_{\infty} = (T_w - T_{\infty})/2$, and the fourth case was TBC-A corresponds to adiabatic upstream wall and step (where T_w is the downstream wall temperature, T_{w1} is the upstream wall and step temperature, and T_{∞} is the free stream temperature). It was found that the recirculation region remains attached to the heated wall downstream of the step when the upstream wall and the step are heated to the same or different uniform temperatures as the downstream wall. The detach of the recirculation region from the heated wall downstream of the step may occur at high buoyancy levels when the upstream wall and step are maintained adiabatic. For higher upstream heating levels, it was found that the reattachment length decreases as the buoyancy level increases. Furthermore, it was noticed that when the upstream wall and the step are heated to a higher temperature than the downstream wall, the velocity distribution downstream of the step may exhibit an overshoot over its free stream value. It was also noticed that the heat transfer from the downstream wall to the fluid decreases as the upstream wall and the step are heated.

Iwai et al. [38] presented a numerical study to investigate the effects of buoyancy-assisting laminar mixed convective flow and thermal fields through a 3D vertical duct having backward-facing step. The downstream wall was maintained to a uniform heat flux, while the rest of the walls were assumed to be adiabatic. The simulations were carried out for buoyancy parameter range between $0 \leq \xi \leq 0.12$, other parameters such as Reynolds number, aspect ratio, expansion ratio, were maintained to be fixed at 125, 16, 2, respectively. Iwai and his coworkers have noticed that 2D are effective in predicting such type of phenomena for buoyancy parameter $\xi \leq 0.06$, for values greater than this, a 3D computational study becomes necessary. The reattachment point and the peak Nusselt number move closer to the step as the buoyancy force increases. Moreover, the secondary recirculation region which developed at the corner between the step and the stepped downstream wall increases in size as the buoyancy force increases. It was found that the maximum Nusselt numbers are located symmetrically near the side walls far from the center plane of the downstream wall. In addition, the maximum Nusselt number was noticed to be downstream of the reattachment point and the distance between them increases with increasing buoyancy force.

The research to study effects of separation and reattachment phenomenon does not concern on laminar flow. Abu-Mulaweh et al. [39] examined the effect of turbulent mixed convection over a 2D vertical backward-facing a step. The step geometry consists of an adiabatic backward-facing step, an upstream wall and a downstream wall heated at constant and uniform temperatures. A free stream air was used as a medium in the velocities range of $0 \leq u_{\infty} \leq 0.41$ m/s for a step height of 22 mm, and a temperature difference ($\Delta T = 30\,^{\circ}\mathrm{C}$) between the heated walls and the free stream. The measurements for different free stream velocities ($u_{\infty} = 0$, 0.23, 0.41 m/s) were carried out at one streamwise location upstream of the step ($x = -5$ cm) and four different streamwise locations downstream of the step ($x = 3.5$, 6, 10, 25 cm). It was indicated that the streamwise velocity increases as the free stream increases and vice versa for the temperature distribution for both upstream and downstream locations. The reattachment length was noticed to be increased with increasing the free stream velocity. The magnitudes for the intensities of streamwise and transverse velocity fluctuations were found to be larger for natural convection than for mixed convection on the upstream location. While, the intensities temperature fluctuations decrease rapidly for mixed convective flow. On the other hand, the magnitudes of the intensities of both velocity and temperature fluctuations are smaller for mixed convection than natural convection at the four downstream locations. It was found that the reattachment length increases while the Nusselt number from the downstream heated wall decreases as the free stream increases, and as a result the location of the maximum heat transfer rate moves away from the step as the free stream velocity increases.

Abu-Mulaweh et al. [40] studied experimentally the effect of the backward-facing step heights on the turbulent mixed convection flow along a 3D vertical flat plate. The experimental setup, step geometry, boundary conditions, and measurement equipments were identical to the previous work done by the same authors in 2001 [39]. The experiments were carried out for step heights of 0, 11, and 22 mm, while the free stream air velocity, u_{∞}, and the temperature difference between the heated walls and free stream, ΔT, were fixed at 0.41 m/s and 30 °C, respectively. Measurements of the flow field were carried out at a location upstream of the step ($x = -5$ cm) at the midplane ($z = 0$) of the plate's width for pure forced, pure natural, and mixed convection flows. It was found that there was a velocity overshoots in the mixed convective case due to the buoyancy assisting near to the heated wall upstream of the step for the dimensionless streamwise velocity distributions. It was observed that increasing the step height enhances the turbulence intensity, which causes the flow to become turbulent downstream of the step. This is because the existence of a backward-facing step triggers transition from the re-laminarized flow upstream of the step to turbulent flow downstream of the step. Furthermore, it was found that as the step height increases, the turbulent intensity of both streamwise and transverse velocity fluctuations, the intensity of the of temperature fluctuations, and heat transfer rate downstream of the step increase. The length of the recirculation region increases with increasing the step height, which results the location of the maximum heat transfer rate moves away from the step as the step height increases.

4. Fundamentals of nanofluids

Heat transfer is commonly encountered in many engineering systems for heating and cooling. The high performance cooling is

essential in many industrial systems such as nuclear plants, HVAC, transportation, energy production, supply to electronics, and paper production. It is also important in consumer products such as computers, car engines, power electronics, and high-powered lasers or X-rays. Traditional fluids are used as coolant and their heat transfer increase with thermal conductivity increment. The development in technologies to perform desired performance, reliable, and minimize size of products reveal to increase in heat loads which in some cases it exceeds 25 kW, therefore liquids and gases have limited thermal performance due to their low thermal conductivity. Many researchers tried to increase the thermal conductivity of the conventional fluids by suspending millimeter- or micrometer-sized solid particles in liquids since the thermal conductivity of solids are higher than liquids. Maxwell [41] made the first effort using millimeter-sized particles suspended in water, but due to the large size and high density the small particles settled out of the suspension.

Many trails have been done to disperse solid particles in liquids since Maxwell's time and all of them observed settlement due to the large size and density of the particles. In 1993, Choi conceived the novel concept of dispersing nanometer-sized particles into base fluids and he proposed the name of Nanofluids in 1995 [42]. Nanofluids are dilute suspensions of nanoparticles smaller than 100 nm, which belong to a new type of functional composite materials. These solid–liquid composites are very stable and show higher thermal conductivity and higher convective heat transfer performance than traditional liquids. Nanofluids have small size which allows them to have less particle sedimentation, erosion, passage clogging, and pressure drop than microfluids or fluids with larger scaled suspensions.

The interest of studying nanofluids have been increased since Choi's concept is presented, and many researches were conducted in different fields and facilities to understand the structures, functions, mechanisms, applications, environmental impacts, and other characteristics of nanofluids. There were some researchers made review papers such as Yu et al. [43], Wang and Mujumdar [44], Li et al. [45], Kakaç and Pramuanjaroenkij [46], Wen et al. [47], Das et al. [48], Wong and Castillo [49], and Nsofor [50]. They declared that nanofluids will produce a new generation of cooling technology, and further researches is needed to improve the stability to avoid cluster phenomena in nanofluids.

4.1. Production of nanoparticles

The invention and improvement of modern technologies permits to fabricate materials with nanometer scale. Many types of materials have been used to make nanoparticles that used in nanofluids. Nanoparticles are synthesized by two different processes which are physical process and chemical process. In physical process, mechanical grinding methods using grinding balls, and the inert-gas-condensation technique were utilized. However, in chemical process many methods are used such as chemical precipitation, chemical vapor deposition, micro-emulsions, spray pyrolysis, and thermal spraying. Carbon nano-tubes (CNTs) and fullerenes are commonly formed in ordinary flames produced by burning methane, ethylene, and benzene, and highly irregular in size and quality in nature. These types of nanoscaled particles are formed by different processes such as arc discharge, laser ablation, chemical vapour deposition, and ball milling.

4.2. Nanoparticle material types

Certain materials have been used to produce nanoparticles and disperse them in host liquids such as oxide ceramics (Al_2O_3, CuO); nitride ceramics (AlN, SiN); carbide ceramics (SiC, TiC); metals (Ag, Al, Au, Cu, Fe); semiconductors (SiO_2, TiO_2); single, double, or multi wall carbon nanotubes (SWCNT, DWCNT, MWCNT); and composite materials such as nanoparticle core-polymer shell composites. Moreover, new materials and structures are desired for use in nanofluids where the solid–liquid interface is doped with various molecules.

4.3. Host liquid types

There are many types of metallic and nonmetallic liquids have been used as host fluid to produce nanofluids. Metallic liquids such as sodium (644 K) have higher thermal conductivity than nonmetallic liquids such as water and organic liquids (ethylene glycol, oil). Water is used as the best traditional liquid due to its high thermal conductivity, abundance, low cost, and friendly to the environment.

5. Preparation of nanofluids

The powder form nanoparticles which disperse in host liquids are called nanofluids. Nanofluids can be produced by two techniques; the two-step (double-step) method, and one-step (single-step) method. These methods have been utilized using different types of chemical and physical techniques to make sure that the solid-liquid mixture is stable to avoid agglomeration, additional flow resistance, possible erosion and clogging, poor thermal conductivity, and poor heat transfer. The two-step method is done by producing the nanoparticles powder initially as introduced in the previous section, and then disperses them into a host liquid. However, in one-step method the nanoparticles are simultaneously made and directly dispersed into the base fluid [51]. It is noticed in the literature that nanofluids with oxide nanoparticles and carbon nanotubes are produced well by the two-step method, while it is not suitable for nanofluids with metallic nanoparticles.

5.1. Techniques of nanofluids production

5.1.1. Two-step technique

It is introduced before that the two-step method is started by nanoparticles production separately and afterward dispersed into a base fluid. The advantage of this method is that it is easily and economically produced. On the other hand, the disadvantage of this method is the quick agglomeration of individual particles before the achievement of complete dispersion due to Vander Waals attractive forces between nanoparticles. This agglomeration is a big obstruction to achieve high heat transfer performance due to the quick settling of particles out of the base fluids and it becomes worse as the volume concentration increases. The agglomeration is not only a problem in nanofluid technology, but it is also a critical issue in all nanopowder technology especially during drying, storage, and nanoparticle transportation stage.

Many different methods have been used to avoid agglomeration using two-step process to initiate the move towards commercialization by facilitating the mass production of nanofluids. Two-step methods such as stirrer, ultrasonic bath, ultrasonic disrupter, and high pressure homogenizer are the popular methods of two-step technique. Eastman et al. [52], Lee at al. [53], and Wang et al. [54] used ultrasonic equipment to disperse Al_2O_3 in the base fluid with less agglomeration. Moreover, Hong et al. [55,56] utilized ultrasonic equipment produced Fe nanofluids by mixing Fe nanocrystalline powder in ethylene glycol. Ultrasonic equipment was also used to produce TiO_2–water nanofluid as introduced in Murshed et al. [57]. Metallic nanofluids were produced by using different two-step methods, but they were not successful due to the high agglomeration. There are some other techniques that are used to attain

the stability of the nanoparticles in the base fluids using the two-step methods such as controlling pH, or adding surfactants and dispersant. These techniques are explained in detail in the next section.

5.1.2. One-step technique

One-step technique is the process of producing nanofluids where the nanoparticles are simultaneously made and directly dispersed into the base fluid. This method is preferable to produce nanofluids containing high thermal conductivity metals to avoid erosion and oxidation of particles. The advantage of this process lies on minimizing of nanoparticles agglomeration. This behavior increases the stability of the suspensions and uniform dispersion in the host liquids. The disadvantage of one-step technique is the limit of quantity of the production due to the slow of the production process, low concentration of nanoparticles, and the high cost.

Different methods have been used to reduce the time and cost using evaporation, physical or chemical one-step methods. The first approach of one-step evaporation method is direct evaporation method which called Vacuum Evaporation onto a Running Oil Substrate (VEROS) technique developed by Akoh et al. [58]. This method was created to produce nanoparticles, but it was found that it is difficult to separate the particles from fluids to produce dry nanoparticles. Later, Wagener et al. [59] proposed a modified VEROS technique using high pressure magnetron sputtering to produce metallic nanofluids such as Ag and Fe. Furthermore, Eastman et al. [52] modified VEROS technique by using direct condensed Cu vapour to form nanoparticles and in contact with flowing with low-vapor pressure ethyl glycol (EG). The well dispersed of Cu nanoparticles in ethyl glycol enhanced the thermal conductivity of the base fluid by up to 40% at the particle volume concentration of 0.3 vol.%. For one-step physical method; a submerged arc nanoparticles synthesis is used in [60–62] to produce nanofluids of Cu, CuO, and TiO_2. In this method, nanoparticles are produced by heating the solid material from an electrode in the form of arc sparkling and condensed into liquid in a vacuum chamber to form nanofluid. Finally, the one-step chemical method is reported by Zhu et al. [63]. They produced Cu nanoparticles of less than 20 nm and dispersed in (EG) by the reduction of a copper salt by sodium hypophosphite under microwave irradiation. A protective polymer and stabilizer called polyvinylpyrrolidone was added so that it inhibited agglomeration. Wei et al. [64] developed a chemical solution method (CSM) to synthesize Cu_2O nanofluids by suspensions of cuprous-oxide (Cu_2O) in water. Their experimental studies showed a substantial thermal conductivity enhancement of up to 24% with their synthesized nanofluids. Among all the three methods; chemical process is the fastest and can be produced in large quantities but it is still not in commercial quantity as in two-step process.

5.2. Stability

The stability of the suspensions in nanofluids is the most critical issue for enhancing heat transfer. This is because nanoparticles tend to aggregate with the time elapsed for its high surface-activity, which results not only the settlement and clogging of microchannels but also the decreasing of thermal conductivity of nanofluids. Nanofluids are considered to be stable when the concentration or particle size of supernatant particles keeps constant. There are some methods have been used to determine the stability of nanofluids such as sedimentation method [65,66], Zeta potential method and absorbency method [67]. Sedimentation method is the most simple and reliable method. It is basically obtained by special apparatus which functioning to measure the variation of concentration or particle size of supernatant particle with sediment time. Moreover, another method using an optical sedimentation photograph to monitor the stability of nanofluids was used but its disadvantage is the long time of the observation compared to other methods. On the other hand, Zeta potential method has a limitation of the viscosity and concentration of nanofluids. A UV–vis spectrophotometer was used to detect the stability of nanofluids. The variation of supernatant particle concentration of nanofluids with sediment time can be obtained by the measurement of absorption of nanofluids because there is a linear relation between the supernatant nanoparticle concentration and the absorbance of suspended particles. It is declared that the most important factors affecting the stability of suspensions were the nanoparticles concentration, additives, viscosity of base liquid and pH value. The variety, diameter, density of nanoparticle and ultrasonic vibration also influence the stability of nanofluids. In addition, the particle morphology, chemical structure of particles and base fluids affect the stability as well. It is observed that the stability of nanofluids do not exceed more than few weeks or months which need to have new techniques to improve the time of nanofluids stability.

6. Experimental investigations on nanofluids

6.1. Thermal conductivity

It is reported that many experimental studies have been done on thermal conductivity of nanofluids because it is a primary assessment of the heat transfer performance of nanofluids. The physical mechanism for thermal conductivity enhancement of nanofluids is not well understood up to date. Maxwell [68] was one of the first investigators who suspended particles thermal conductivity. He used a very dilute suspension of spherical particles by ignoring the interactions between the particles, and made an equation that can be applied only to mixtures with low particle volume concentrations. The gap of particles interactions attracts many researchers to extend or improve the Maxwell equation with various factors that affect thermal conductivity such as particle shape [69–77], particle dispersion and distribution [78], volume concentration [79–82], particle-shell structure [69,83–88], and contact resistance [89,90]. Even though these studies tried to improve equations to predict thermal conductivity but the comparison between the experimental data and theoretical predictions for nanofluids is generally not satisfactory. New techniques of mechanism have been used to improve the prediction of nanoscale such as nanoparticle-matrix interfacial layer [91–94], nanoparticle Brownian motion [95–99], and nanoparticle cluster/aggregate [100,101].

6.1.1. Thermal conductivity measurement methods

There are many methods used to measure nanofluids thermal conductivity such as transient hot-wire (THW), temperature oscillation (TO) and steady-state (SS) methods [55–57,61,102–105]. Transient hot-wire method is well established as the most accurate, reliable and robust measurement technique for the thermal conductivity of nanofluids, and so it is utilized in most of thermal conductivity measurements. The transient hot-wire is functioned as both heater and thermometer and many modifications have been proposed such as coating the hot wire. In oscillation method; the electrical components are removed from the test sample and perform as purely thermal as reported by [106–108], so that the ion movement is not affecting the measurements. The steady-state method was used by [54,109] to measure the effective thermal conductivity of Al_2O_3 and CuO nanofluids with an improvement of 12% in thermal conductivity enhancement at 3% volume fraction of nanoparticles.

6.1.2. Effects of thermal conductivity parameters

Many experimental studies have been done by different researchers for examining and improving the thermal conductivity enhancement of certain types of nanofluids using different

methods and parameters. They calculated the thermal conductivity enhancement by using the ratio of the thermal conductivity of the nanofluid over its base fluid thermal conductivity. It is noticed that most of the studies did not concerned or noticed the particle size distribution. In addition, the effect of the particles agglomeration in the base fluid is also unknown.

It is declared that the thermal conductivity of nanofluid is sensitive to certain parameters which are responsible for constant nanofluids such as particle volume concentration, particle size, particle material, particle shape, base fluid material, temperature, additives and surfactants, and acidity. These parameters will be introduced in the following section separately base on the previous experimental investigations and findings.

6.1.2.1. Effects of particle volume concentration. One of the most important parameters is volume concentration or in other words volume fraction. It is the ratio of the volume of nanoparticles to the base fluid volume. As declared previously that solids have higher thermal conductivity than liquids, so as the percentage of nanoparticles increases, the thermal conductivity increases as well. Unfortunately, this is not working for all cases; it is declared that many colloidal and biological suspensions show strong non-Newtonian behavior but nanofluids with volume concentration not more than 5% exhibit Newtonian behavior. At higher particle volume concentrations, the increase in enhancement is expected to diminish or even reverse, and nanofluid viscosity would increase. Three methods have been used by Wang et al. [54] to measure the viscosity of nanofluids but they did not observe any non-Newtonian effects. They used Al_2O_3–water nanofluid and found a 30% increase in viscosity when compared with pure water at 3% volume concentration of the particles. However, Pak and Cho [110] measured the viscosity to be much higher. There are many researches done on particle volume concentration [42,54,102,106,109,111–126] for different particle size, particle shape, particle material, base fluid material, additive, and acidity level. They reported that at low volume concentration (<5%) the thermal conductivity ratios increase linearly with volume concentration. Furthermore, it is noticed that metallic nanofluids and either single- or multi-wall nanotubes enhance thermal conductivity with low volume concentration compared to oxides and nonmetallic nanofluids.

6.1.2.2. Effects of particle size. The size of particle plays a significant role in thermal conductivity and heat transfer enhancement in base fluids. As introduced before that different suspension sizes of millimeter and micrometer particles in host liquid have been used to increase the thermal conductivity, but the particles agglomerate quickly and settled out of the liquid. Nanoparticles are formed to decrease the size of the particles so that the time of sedimentation decreases to reach in some cases to more than few weeks or months. The size of nanoparticles are in the range of 1–100 nm and as the size decreases the thermal conductivity increases due to the increase of the relative surface area [127]. The much larger relative surface area of nanoparticles, should not only significantly improve thermal conductivity capabilities, but also should increase the stability of the suspensions. In addition, it is reported that as the size of nanoparticle reduced, the Brownian motion will be induced [128]. Furthermore, there are some researches indicate that the thermal conductivity enhanced with nanoparticles increment to ≈60nm and vice versa for greater values [53,114]. The size of nanoparticles in the host liquid is too important to the modern science and technology. It can be applied in small size systems such as micro-channels and nanosystems where the clog and erosion is prohibited.

6.1.2.3. Effects of particle material. There are many types of materials have been utilized to produce nanofluids such as oxide ceramics (Al_2O_3, CuO); nitride ceramics (AlN, SiN); carbide ceramics (SiC, TiC); metals (Ag, Al, Au, Cu, Fe); semiconductors (SiO_2, TiO_2); single, double, or multi wall carbon nanotubes (SWCNT, DWCNT, MWCNT); and composite materials. It was found that metallic and allotrops of carbon nanoparticles (such as diamond) increase the thermal conductivity of a host fluid more than other types of nanoparticles having the same volume concentration.

6.1.2.4. Effects of particle shape. Thermal conductivity enhancement in nanofluids is affected by the geometrical shape of the particles. Different shapes such as spherical and cylindrical (fiber, rod, and tube) nanoparticles have been used in different host liquids to identify the enhancement of nanofluids thermal conductivity. It is reported that cylindrical nanoparticles are better than spherical shape in enhancing the thermal conductivity of nanofluids [57,129]. This is due to the elongated particles and the large aspect ratio of the surface area to volume that conducts heat through the fluid.

6.1.2.5. Effects of base fluid material. Many host liquids have been used to produce nanofluids such as aqueous and organic liquids (ethylene glycol, and oils) to enhance thermal conductivity. It is found that the thermal conductivity enhancement increases as the thermal conductivity of the base fluid decreases [114,115,130].

6.1.2.6. Effects of temperature. The nature of the nanofluid thermal conductivity is sensitive to temperature. Many studies have been done for the effect of temperature on thermal conductivity. They reported that the thermal conductivity enhanced as the temperature increases due to the motion of the nanoparticles [106,109,127,131]. In opposite, Masuda et al. [111] found that the thermal conductivity enhancement decreases as the temperature increases.

6.1.2.7. Effects of additives and surfactants. It is declared that certain types of additive have been used in nanofluids to keep nanoparticles in suspension form and prevent agglomeration for improving the thermal conductivity enhancement. The additives types and concentration is added depend on the type of both nanoparticles and base fluids. Eastman et al. [113] used thloglycolic acid in Cu-ethyl glycol, Assael et al. [132] used CTAB and Nanosperse AQ for MWCNT-water, Ding et al. [122] gum Arabic for MWCNT-water, and other types of acidic fluids such as Oleic acids, etc.

6.1.2.8. Effects of Acidity (PH). Limited studies have been published on the effect of fluid acidity on the thermal conductivity enhancement of nanofluids [117,126]. But the general trend is that acidity increases the thermal conductivity enhancement.

6.1.3. Mechanisms of thermal transport in nanoscale

6.1.3.1. Brownian motion. Brownian motion is one of the parameters that affect the flow and heat transfer of nanofluids. It is basically the random dynamic mode of particles in a liquid where the particles collide between each other. It was determined that the thermal conductivity increases with an increase in temperature, but also it was shown that nanofluids compose of smaller particles experienced greater enhancement than with larger particles. Since temperature represents the overall kinetic energy of the particles, an increase in temperature will cause increase in the particles motion. It is easier for smaller particles to move; therefore, smaller particles will display a higher level of Brownian motion than larger particles. It is outlined that the movement of nanoparticles due to Brownian motion was too slow in transporting heat through a fluid and it can be ignored [133–136]. To travel from one point to another, a particle moves a large distance over many different paths in order to reach a destination that may be a short distance from the starting point. Therefore,

the random motion of particles, no matter how agitated or energetic they may be not a key factor in the improvement of heat transfer. On the other hand, there are some studies developed a dynamic model that takes into account convection heat transfer induced by Brownian nanoparticles. They reported that Brownian motion of nanoparticles at the molecular and nanoscale levels is a main mechanism controlling the thermal conductivity of nanofluids [96,98,137].

6.1.3.2. Liquid layering on the nanoparticle–liquid interface. There are some studies declared that there is a liquid layering on the nanoparticles, which improves the enhancement of nanofluid heat transfer properties. The thickness and thermal conductivity of the nanolayer are not known yet, but the liquid molecules close to a solid surface have been proven by Yu et al. [138] to form layers. Ren et al. [94] indicated that the thermal conductivity increases with liquid layer increment. They assumed that the thermal conductivity of the layer would be somewhere between the thermal conductivity of the bulk fluid and the nanoparticle. On the other hand, Keblinski [135] assumed that the thermal conductivity of the interfacial liquid is the same as that of the solid and showed that the resultant large effective volume of the particle–layered–liquid structure would enhance the thermal conductivity. Ren et al. [94] also found that as the nanoparticles increased in size, the effects of the liquid layering became weaker. Yu and Choi [92] determined that the solid–liquid interfacial layers in the nanofluid plays an important role in the enhanced thermal conductivity especially when the particle diameter is less than 10 nm.

6.1.3.3. Nature of heat transport in nanoparticles. Heat is transferred via conduction implies that heat is transferred internally, by vibrations of atoms and molecules. The vibrations of the atoms which are connected together as give rise to the vibrations of the whole crystal, that is, to lattice vibrations. The energy of the whole vibrating system is quantized, and the quantum of thermal energy absorbed or emitted by an atom is called a phonon. Therefore, a phonon is essentially a quantized mode of vibration occurring in rigid crystal lattice and plays a major role in material's thermal conduction. Keblinski [135] demonstrated that the phonon mean free bath is much shorter in the liquid than in the particle and would be effective as the distance between the particles and the thickness of the layered liquid are small. A greater phonon density exists in hot regions of a crystal than in cooler regions. Therefore, heat conduction is essential due to the diffusion of phonons, and because the temperature gradient changes from hot to cold regions. Electrons can also carry heat; thus, metals have many free electrons which move around randomly, heat can be transferred from one part of the metal to another quite effectively. That is why metals are generally very good conductors of heat.

6.1.3.4. Effects of nanoparticles clustering. Clustering of particles is one of the major problems that affects the enhancement of thermal conductivity by creating path of lower thermal resistance. It is noticed that as the particles agglomerate increases, the size increases and becomes denser where they clustered down, and end with low thermal conductivity enhancement. To avoid or minimize the particles clustering, nanofluids should consist of low volume concentration and small particles size. The effective volume of a cluster, which is the volume from which other clusters are excluded, can be much larger than the physical volume of the particles [135,136]. The effective volumetric concentration of the particles, inside a cluster, is larger than the volume of the solid phase, since within such cluster heat can move very rapidly.

6.1.3.5. Thermophoresis. Thermophoresis refers to the motion of colloidal particles in response to a temperature gradient which can be clarified by applying the kinetic theory. The high energy molecules in the hot region of the liquid impinge on the particles with greater momentum than do molecules coming from the cold region, thus leading to the migration of the particles in the direction opposite to the temperature gradient. This mechanism has been found to be negligible, primarily because of the very small particle migration velocity [91,136].

6.1.3.6. Reduction in thermal boundary layer thickness. A few numbers of researches have been done for studying the thermal boundary layer such as in Ding et al. [139]. They mentioned that a reduction in the thermal boundary layer thickness may be a mechanism that causes heat transfer enhancements in nanofluids. It is still needed to have more research on this mechanism to understand its effects in nanofluids convective heat transfer.

6.2. Viscosity

Nanofluids are expected to be used under flow conditions and the flow of suspension which are sometimes drastically different from that of most common heat transfer fluids that have Newtonian characteristics, so it is essential to have the rheological properties of nanofluid to use practically. Rheological properties can provide the knowledge on the microstructure under both static and dynamic conditions, which are important to understand the mechanism of heat transfer enhancement using nanofluids. Fluids have frictional forces between the molecules and, therefore, they display a certain flow resistance which can be measured as viscosity. The fluids are either Newtonian or non-Newtonian, depends on their viscosity. It has been demonstrated by Newton that the shear force acting on a liquid is proportional to the resulting flow velocity. If the viscosity of the fluid remains constant with an increase in shear rate, it is called Newtonian fluid, but if the viscosity changes with an increase in shear rate, it is called non-Newtonian fluid. The shear viscosity of samples displaying shear-thickening behavior is dependent on the degree of shear load. However, the viscosity increases with an increase in shear stress. It is declared that the viscosity of nanofluids is mainly dependent on volume concentration, nanoparticle size, and temperature [140–148]. Nanofluids with high concentration and large size nanoparticles have high particle interaction and may result in particles agglomeration and thus increase the flow resistance and decrease the heat transfer enhancement. Particle shape plays an important role since during the shear process, particles rotate as they move. Cube-shape particles take up more volume when rotating than spherical particles and hence less free volume is available for the liquid between the particles. In addition, it was reported that the viscosity decreases with temperature increment.

6.3. Heat capacity

The heat capacity of a substance is the amount of heat required to change its temperature by one Kelvin, and has units of joule per Kelvin (J/K) in the SI system. The specific heat capacity is essentially the heat capacity per unit mass, usually per gram of material (J/g K). The specific heat capacities of nanofluids are different from that of base fluid and increase with the size and volume concentration of nanoparticles decrement. The high specific interfacial area of nanoparticle can absorb liquid molecules to its surface and form liquid layers, which will reversely constrain nanoparticle and turns its free boundary surface atoms to be non-free interior atoms. This effect will also increase the specific heat capacity of nanofluid [149–153].

7. Applications of nanofluids

Nanofluids could be used as a super coolant in many industrial and consumer products such as nuclear reactors, car engines, radiators, computers, X-rays, and many other applications. It is called super-coolant because it can absorb heat more than any traditional fluids, so it can minimize the size of system and increase its performance. Most of the researches were concerned on studying the properties, parameters, and heat transfer enhancement, but not much research done for commercial systems. Some researchers tried to apply nanofluids in real systems and observe their flow and heat transfer. Tzeng et al. [154] studied the effect of nanofluids when used as engine coolants. CuO (4.4 wt%) and Al_2O_3 (4.4 wt%) nanoparticles and antifoam were individually mixed with automatic transmission oil, and experiment them by a real drive of four-wheel-drive (4WD) transmission system. The experimental results showed that, the antifoam–oil provided the highest temperature distribution in rotary blade coupling and, accordingly, the worst heat transfer effect, and CuO–oil provided the lowest temperature distribution both at high and low rotating speed and, accordingly, the best heat transfer effect. Chein and Huang [155] used Cu nanofluid with various concentrations to study silicon microchannel heat sink performance. They found that nanofluid cools better than pure water and observed no extra pressure drop because of small particle size and low particle volume fraction. Koo and Kleinstreuer [156] used two types of nanofluids (i.e., CuO nanospheres at low volume concentrations in water and in ethylene glycol) for the conjugate heat transfer problem for microheat sinks. The effect of Brownian motion on the effective fluid viscosity was considered and found to be less significant than that on the effective thermal conductivity. Many other industrial and consumer companies have their own researches using nanofluids such as medical equipments, computer manufacturing, and gas and oil [157].

8. Safety

Up to date the behavior, parameters and mechanisms of nanofluids are not clearly understood, and because of these variables scientists still cannot accurately predict how nano-materials will affect living organisms. Now, it is just clear that the biological activity and biokinetics of nanoparticles are different from larger particles, and that they depend on many parameters. These parameters can modify cellular uptake, protein binding, translocation from portal of entry to target site, and the possibility of tissue injury. Several studies have demonstrated that nanoparticles are more toxic than micro-particles of the same material.

9. Environmental effects

Nanofluids are observed to be an environmental friend due to its high heat transfer enhancement. The usage of nanofluids decreases the consumption of fuel in engines, and electricity which are the highest pollutants that threat our earth and increase its temperature. It is noticed that if nanofluids improve chiller efficiency by 1%; it will save 320 billion kwh of electricity or equivalent to 5.5 million barrels of oil per year just in USA alone.

10. Convective heat transfer of nanofluids

Convective heat transfer is the phenomena of the macroscopic motion of the fluid relative to the surface due to the heat transfer between them. The surface could be a solid wall or an interface with another liquid. Convective heat transfer is divided into two major types, which are natural convective heat transfer where fluid motion is induced by buoyancy, and forced convective heat transfer where fluid is forced to flow through a boundary region. Convective heat transfer of a medium depends on its thermophysical properties such as, thermal conductivity, specific heat capacity, viscosity, density, and thermal expansion coefficient.

10.1. Natural convection

The natural convection studies using nanofluids are very few. Even though the research is limited, however the available results are diverged. Putra et al. [158], and Wen and Ding [120] made an experimental investigation for natural convection using Al_2O_3 and TiO_2 nanofluids, respectively. They found that the presence of nanoparticles in water systematically decreased the natural convective heat transfer coefficient. Furthermore, they declared that the decrease was due to the effects of particle/fluid slip and sedimentation of nanoparticles. In contrast, Khanafer et al. [159] used a numerical technique and predicted that nanofluids enhanced natural convective heat transfer. It is needed to do more research on natural convection to get a clear view and well understanding for such phenomena.

10.2. Forced convection

Forced convection studies using nanofluids are also limited and they have diverged results from each other. Majority of forced convective heat transfer using nanofluids found that there is convective heat enhancement such as Li and Xuan [160], Xuan and Li [161], Lee and Choi [162], Jang and Choi [163], and Xuan and Roetzel [164]. There are some studies reported that heat transfer can be enhanced under certain conditions (such as low volume concentration for decreasing the viscosity) by Pak and Cho [165], Lee and Mudawar [166], and Chein and Chuang [167]. A very few studies show a decrease in the convective heat transfer coefficient when nanoparticles are added to the base liquids such as Yang et al. [168].

10.3. Convection of nanofluids in BFS

It is noticed in the literature that there are few experimental and numerical studies have been done to investigate the flow and heat transfer of nanofluids in different geometries with different regimes. Engineering geometries such as tubes and annuli were the first geometries that have been used for investigating nanofluids enhancement. Most of the studies show that nanofluids have higher thermal transport than any ordinary fluids and their enhancement increase or decrease depends on the change of the parameters and characteristics which introduced in the previous sections. Other studies have been done to apply nanofluids for microchannels, different geometrical shapes, and systems. The results show an improvement in thermal transport enhancement.

To the best knowledge of the authors, there is only one paper investigated the flow and heat transfer influence of nanofluids through a duct with backward facing step. Abu-Nada [169] studied the flow and heat transfer influences over a backward facing step (BFS) using nanofluids numerically. Different volume fractions and types of nanoparticles were used in the base fluid (water) and flowed through BFS channel with an expansion ratio ER = 2. The Reynolds number and nanoparticles volume fraction used were in the range of $200 \leq Re \leq 600$ and $0 \leq \varphi \leq 0.2$, respectively. The Prandtl number of the base fluid was kept constant at 6.2 for the five types of nanoparticles which are Cu, Ag, Al_2O_3, CuO, and TiO_2. It was noticed that at the top wall and for $Re = 200$, an enhancement in the Nusselt number was registered by increasing the volume fraction of the nanoparticles. Moreover, there was an enhancement in Nusselt number at the top wall for $Re > 300$ except in the secondary recirculation zone where insignificant enhancement was

Table 2
Summary of the parameters that affect the flow over backward-facing step.

	As the parameter increases							
	Step height	Velocity	Inclination	Prandtl number	Expansion Ratio	Aspect ratio	Buoyancy-assisting	Buoyancy-opposing
Local Nusselt number	Increases	Increases	Decrease, $0^\circ \leq \phi \leq 180^\circ$ Increase, $180^\circ \leq \phi \leq 360^\circ$	Increases	Decreases	Increases	Increases	Decreases
Reattachment length	Increases	Increases	Increases, $0^\circ \leq \phi \leq 180^\circ$ Decrease, $180^\circ \leq \phi \leq 360^\circ$	Increases	$R < 2.25$, increase $R > 2.25$, decrease	Increases	Increases	Decreases

registered. It was found that the high Nusselt number inside the recirculation zone is mainly depended on the thermophysical properties of the nanoparticles and it is independent on of Reynolds number. Both the Reynolds number and thermophysical properties of the nanoparticles have an influence on the value of Nusselt number outside the recirculation region. However, it was noticed that outside the recirculation zone, nanoparticles having high thermal conductivity (such as Ag or Cu) have more enhancements on the value of the Nusselt number, and verse visa in the primary and secondary recirculation zones.

Very recently, the same authors [170–172] investigated numerically the laminar forced and mixed convection assisting flow over horizontal and vertical backward-facing steps in a duct using different nanofluids (such as Au, Ag, Al_2O_3, Cu, CuO, diamond, SiO_2, and TiO_2). It was found that a primary recirculation region developed after the sudden expansion and it starts to become fully developed downstream of the reattachment point. The reattachment point is found to move downstream far from the step as Reynolds number increases. Moreover, they also inferred that low density nanofluids have higher absolute velocity compared to high density nanofluids. It is found that a recirculation region was developed straight behind the backward facing step which was appeared between the edge of the step and few millimeters before the corner which connects the step and the downstream wall. In a few millimeters zone between the recirculation region and the downstream wall; a U-turn flow was developed opposite to the recirculation flow which is mixed with the unrecirculated flow and travels along the channel. Two maximum and one minimum peaks in Nusselt number were observed along the heated downstream wall. It is inferred that Au nanofluid has the highest maximum peak of Nusselt number, while diamond nanofluid has the highest minimum peak in the recirculation region. Nanofluids with higher Prandtl number have higher maximum peak of Nusselt numbers after the separation and recirculation flow is vanished.

11. Conclusions

In this article, a comprehensive review of previous efforts is presented for different convective flow regimes and heat transfer through a duct having backward facing step. The effects of several parameters in geometry, boundary conditions, and types of fluids were extensively introduced and investigated. In backward-facing step, the Nusselt number increases as the parameter such as step height, velocity, Prandtl number, and aspect ratio increase, and a vice versa for expansion ratio. It was reported that the reattachment length increases as step height, velocity, Prandtl number, aspect ratio, and expansion ratio less than 2.25 increase, and decreases with increasing expansion ratio greater than 2.25. These features are summarized in Table 2. In addition, an extensive review for preparation, parameters, mechanisms, characteristics, convective heat transfer enhancement, applications, safety, and environmental impacts for nanofluids was also reported. It is found that nanofluids will solve many technological problems and space limitation, and will be used commercially such as other ordinary coolants in the future. It was observed from the literature review that many work have been done using conventional fluids to study the heat transfer and fluid flow characteristics in BFS. Thus, more work using nanofluids is needed to investigate the heat transfer enhancement over backward facing step.

References

[1] Blackwell BF, Pepper DW. Benchmark problems for heat transfer codes. In: Proceedings of the HTD-ASME Winter Annual Meeting, vol. 222. 1992. Anaheim 1–89.
[2] Blackwell BF, Armaly BF. Computational aspect of heat transfer benchmark problems. In: ASME Winter Annual Meeting, HTD, vol. 258. 1993.

[3] Blackwell BF, Armaly BF. Benchmark problem definition and summary of computational results for mixed convection over a backward-facing step. In: ASME Winter Annual Meeting, HTD, vol. 258. 1993. pp. 1–10.
[4] Abu-Mulaweh HI. A review of research on laminar mixed convection flow over backward- and forward-facing steps. Int J Therm Sci 2003;42:897–909.
[5] Barbosa Saldana JG, Anand NK, Sarin V. Numerical simulation of mixed convective flow over a three-dimensional horizontal backward facing step. J Heat Transfer 2005;127:1027–36.
[6] Goldstein RJ, Ericsen VL, Olson RM, Eckert ERG. Laminar separation reattachment, and transition of the flow over a downstream-facing step. J Basic Eng 1970;92:732–41. D (4).
[7] Denham MK, Patrick MA. Laminar flow over a downstream-facing step in a two-dimensional flow channel. Trans Inst Chem Eng 1974;52:361–7.
[8] Armaly BF, Durst F, Pereira JCF, Schonung B. Experimental and theoretical investigation of backward-facing step flow. J Fluid Mech 1983;127:473–96.
[9] Armaly BF, Durst F, Kottke V. Momentum heat and mass transfer in backward-facing step flows, Numerical Heat Transfer and Fluid Flow. New York: Mc Graw-Hill; 1980.
[10] Shih C, Ho CM. Three-dimensional recirculation flow in a backward facing step. J Fluids Eng 1994;116:228–32.
[11] Chiang TP, Sheu TWH, Tsai SF. Topological flow structures in backward-facing step channels. Comput Fluids 1997;26(4):321–37.
[12] De Brederode V, Bradshaw P. Three-dimensional flow in normally two-dimensional separation bubbles i. flow behind a rearward-facing step. I. C Aero Report 1972; p. 72–79.
[13] Hertzberg J, Ho CM. Vortex dynamics in a rectangular sudden expansion. AIAA J 1992;30(10):2420–5.
[14] Tylli N, Kaiktsis L, Ineichen B. Sidewall effect in flow over a backward-facing step: experiments and numerical simulations. Am Inst Phys 2002;14:3835–45.
[15] Armaly BF, Li A, Nie JH. Measurements in three-dimensional laminar separated flow. Int J Heat Mass Transfer 2003;46:3573–82.
[16] Nie JH, Armaly BF. Reverse flow regions in three-dimensional backward-facing step flow. Int J Heat Mass Transfer 2004;47:4713–20.
[17] Aung W. An experimental study of laminar heat transfer downstream of back-step. J Heat Transfer 1983;105:823–9.
[18] Sparrow EM, Chuck W. PC solutions for the heat transfer and fluid flow downstream of an abrupt, asymmetric enlargement in a channel. Numer Heat Transfer 1987;12:19–40.
[19] Khanafer K, Al-Azmi B, Al-Shammari A, Pop L. Mixed convection analysis of laminar pulsating flow and heat transfer over a backward-facing step. Int J Heat Mass Transfer 2008;51:5785–93.
[20] Chen YT, Nie JH, Armaly BF, Hsieh H. Turbulent separated convection flow adjacent to backward-facing step-effects of step height. Int J Heat Mass Transfer 2006;49:3670–80.
[21] Iwai H, Nakabe K, Suzuki K. Flow and heat transfer characteristics of backward-facing step laminar flow in a rectangular duct. Int J Heat Mass Transfer 2000;43:457–71.
[22] Nie JH, Armaly BF. Three-dimensional convective flow adjacent to backward-facing step-effects of step height. Int J Heat Mass Transfer 2002;45:2431–8.
[23] Armaly BF, Li A, Nie JH. Three-dimensional forced convection flow adjacent to backward-facing step. J Thermophys Heat Transfer 2002;16:222–7.
[24] Barbosa Saldana JG, Anand NK. Forced convection over a three-dimensional horizontal backward facing step. Int J Comput Methods Eng Sci Mech 2005;6(4):225–34.
[25] Lan H, Armaly BF, Drameier JA. Three-dimensional simulation of turbulent forced convection in a duct with backward-facing step. Int J Heat Mass Transfer 2009;52:1690–700.
[26] Lin JT, Armaly BF, Chen TS. Mixed convection heat transfer in inclined backward-facing step flows. Int J Heat Mass Transfer 1991;34(6):1568–71.
[27] Lin JT, Armaly BF, Chen TS. Heat transfer in buoyancy-assisted, vertical backward-facing step flow. Int J Heat Mass Transfer 1990;33:2121–32.
[28] Hong B, Armaly BF, Chen TS. Laminar mixed convection in a duct with a backward-facing step: the effects of inclination angle and prandtl number. Int J Heat Mass Transfer 1993;36(12):3059–67.
[29] Abu-Mulaweh HI, Armaly BF, Chen TS. Measurements of laminar mixed convection in boundary-layer flow over horizontal and inclined backward-facing steps. Int J Heat Mass Transfer 1993;36(7):1883–95.
[30] Iwai H, Nakabe K, Suzuki K, Matsubara K. The effects of duct inclination angle on laminar mixed convective flows over a backward-facing step. Int J Heat Mass Transfer 2000;43:473–85.
[31] Lin JT, Armaly BF, Chen TS. Mixed convection in buoyancy-assisting, vertical backward-facing step flows. Int J Heat Mass Transfer 1990;43(10):2121–32.
[32] Aung W, Worku G. Theory of fully developed, combined convection including flow reversal. J Heat Transfer 1985;108:485–8.
[33] Hong B, Armaly BF, Chen TS. Mixed convection in a vertical duct with a backward-facing step: uniform wall heat flux case, in: fundamental of mixed convection. In: ASME Winter Annual Meeting, HTD, vol. 213. 1992. p. 73–8.
[34] Baek BJ, Armaly BF, Chen TS. Measurements in buoyancy-assisting separated flow behind a vertical backward-facing step. J Heat Transfer 1993;115:403–8.
[35] Abu-Mulaweh HI, Armaly BF, Chen TS. Measurements in buoyancy-assisting laminar boundary layer flow over a vertical backward-facing step-uniform wall heat flux case. Exp Therm Fluid Sci 1993;7:39–48 (1993).
[36] Abu-Mulaweh HI, Armaly BF, Chen TS. Measurements in buoyancy-opposing laminar flow over a vertical backward-facing step. J Heat Transfer 1994;116:247–50.
[37] Abu-Mulaweh HI, Armaly BF, Chen TS. Effects of upstream wall heating on mixed convection in separated flows. J Thermophys Heat Transfer 1995;9:715–21.
[38] Iwai H, Nakabe K, Suzuki K, Mastubara K. Numerical simulation of buoyancy-assisting backward-facing step flow and heat transfer in a rectangular duct. Heat Transfer Asian Res 1999;28:58–76.
[39] Abu-Mulaweh HI, Armaly BF, Chen TS. Turbulent mixed convection flow over a backward-facing step. Int J Heat Mass Transfer 2001;44:2661–9.
[40] Abu-Mulaweh HI, Armaly BF, Chen TS. Turbulent mixed convection flow over a backward-facing step-the effect of step heights. Int J Heat Fluid Flow 2002;23:758–65.
[41] Maxwell JC. A treatise on electricity and magnetism. second ed. Oxford, UK: Clarendon Press; 1881.
[42] Choi SUS. Enhancing thermal conductivity of fluids with nanoparticles, Developments and Applications of Non-Newtonian Flows, FED-231/MD-66, 1995; p. 99–105.
[43] Yu W, France DM, Routbort JL, Choi SUS. Review and comparison of nanofluid thermal conductivity and heat transfer enhancements. Heat Transfer Eng 2008;29(5):432–60.
[44] Wang XQ, Mujumdar AS. Heat transfer characteristics of nanofluids: a review. Int J Therm Sci 2007;46:1–19.
[45] Li Y, Zhou J, Tung S, Schneider E, Xi S. A review on development of nanofluid preparation and characterization. Powder Technol 2009;196:89–101.
[46] Kakaç S, Pramuanjaroenkij A. Review of convective heat transfer enhancement with nanofluids. Int J Heat Mass Transfer 2009;52:3187–96.
[47] Wen D, Lin G, Vafaei S, Zhang K. Review of nanofluids for heat transfer applications. Particuology 2009;7:141–50.
[48] Das SK, Choi SUS, Patel HE. Heat transfer in nanofluids: A review. Heat Transfer Eng 2006;27(10):3–19.
[49] Wong KV, Castillo MJ. Heat transfer mechanisms and clustering in nanofluids. Adv Mech Eng 2010;10, 1155 (795478) 9 p.
[50] Nsofor EC. Recent patents on nanofluids (Nanoparticles in liquids) heat transfer. Recent Patents Mech Eng 2008;1:190–7.
[51] Hwang Y, Lee JK, Lee JKu, Jeong YM, Cheong SI, Ahn YC, et al. Production and dispersion stability of nanoparticles in nanofluids. Powder Technol 2008;186:145–53.
[52] Eastman JA, Choi US, Li S, Thompson LJ, Lee S. Enhanced thermal conductivity through the development of nanofluids. In: Materials Research Society Symposium-Proceedings 457 Materials Research Society. 1997. p. 3–11.
[53] Lee S, Choi SUS, Li S, Eastman JA. Measuring thermal conductivity of fluids containing oxide nanoparticles. J Heat Transfer 1999;121:280–9.
[54] Wang X, Xu X, Choi SUS. Thermal conductivity of nanoparticle-fluid mixture. J Thermophys Heat Transfer 1999;13(4):474–80.
[55] Hong TK, Yang HS, Choi CJ. Study of the enhanced thermal conductivity of Fe nanofluids. J Appl Phys 2005;97:1–4 (064311).
[56] Hong KS, Hong TK, Yang HS. Thermal conductivity of Fe nanofluids depending on the cluster size of nanoparticles. Appl Phys Lett 2006;88(31901):1–3.
[57] Murshed SMS, Leong KC, Yang C. Enhanced thermal conductivity of TiO_2–water based nanofluids. Int J Therm Sci 2005;44(4):367–73.
[58] Akoh H, Tsukasaki Y, Yatsuya S, Tasaki A. Magnetic properties of ferromagnetic ultrafine particles prepared by vacuum evaporation on running oil substrate. J Crystal Growth 1978;45:495–500.
[59] Wagener M, Murty BS, Gunther B. Preparation of metal nanosuspensions by high-pressure DC-sputtering on running liquids. In: Komarnenl S, Parker JC, Wollenberger HJ, editors. Nanocrystalline and Nanocomposite Materials II 457 Materials Research Society, Pittsburgh, PA. 1997. p. 149–154.
[60] Chang H, Tsung TT, Chen LC, Yang YC, Lin HM, Lin CK. Nanoparticle suspension preparation using the Arc spray nanoparticle synthesis system combined with ultrasonic vibration and rotating electrode. Int J Adv Manuf Technol 2005;26:552–8.
[61] Lo CH, Tsung TT, Chen LC, Su CH, Lin HM. Fabrication of copper oxide nanofluid using submerged Arc Nanoparticle Synthesis System (SANSS). J Nanopart Res 2005;7:313–20.
[62] Lo CH, Tsung TT, Chen LC. Shaped-controlled synthesis of Cu-based nanofluid using submerged Arc Nanoparticle Synthesis System (SANSS). J Crystal Growth 2005;277:636–42.
[63] Zhu HT, Lin YS, Yin YS. A novel one-step chemical method for preparation of copper nanofluids. J Colloid Interface Sci 2004;277:100–3.
[64] Wei X, Zhu H, Kong T, Wanga L. Synthesis and thermal conductivity of Cu_2O nanofluids. Int J Heat Mass Transfer 2009;52:4371–4.
[65] Hwang Y, Park HS, Lee JK, Jung WH. Thermal conductivity and lubrication characteristics of nanofluids. Curr Appl Phys 2006:67–71, 6S1.
[66] Hwang Y, Lee JK, Lee CH, Jung YM, Cheong SI, Lee CG, et al. Stability and thermal conductivity characteristics of nanofluids. Thermochim Acta 2007;455: 70–4.
[67] Li X, Zhu D, Wang X. Evaluation on dispersion behavior of the aqueous copper nano-suspensions. J Colloid Interface Sci 2007;3(10):456–63.
[68] Maxwell JC. Treatise on electricity and magnetism. Oxford, UK: Clarendon Press; 1873.
[69] Fricke H. A mathematical treatment of the electric conductivity and capacity of disperse systems, I: The Electric Conductivity of a Suspension of Homogeneous Spheroids. Phys Rev 1924;24:575–87.
[70] Fricke H. The Maxwell–Wagner dispersion in a suspension of ellipsoids. J Phys Chem 1935;57:934–7.
[71] Polder D, van Santen JH. The effective permeability of mixtures of solids. Physica 1946;12:257–71.

[72] Hamilton RL, Crosser OK. Thermal conductivity of heterogeneous two-component systems. Ind Eng Chem Fundam 1962;1:187–91.
[73] Taylor LS. Dielectrics properties of mixtures. IEEE Trans Antennas Propag 1965;13:943–7.
[74] Taylor LS. Dielectrics loaded with anisotropic materials. IEEE Trans Antennas Propag 1966;14:669–70.
[75] Granqvist CG, Hunderi O. Optical properties of ultrafine gold particles. Phys Rev B 1977;16:3513–34.
[76] Granqvist CG, Hunderi O. Conductivity of inhomogeneous materials: effective-medium theory with Dipole–Dipole interaction. Phys Rev B 1978;18:1554–61.
[77] Xue Q. Effective-medium theory for two-phase random composite with an interfacial shell. J Mater Sci Technol 2000;16:367–9.
[78] Rayleigh L. On the influence of obstacles arranged in rectangular order upon the properties of a medium. Philos Mag 1892;34:481–502.
[79] B¨ottcher CJF. The dielectric constant of crystalline powders. Recueil des Travaux Chimiques des Pays-Bas 1945;64:47–51.
[80] Landauer R. The electrical resistance of binary metallic mixtures. J Appl Phys 1952;23:779–84.
[81] Jeffrey DJ. Conduction through a random suspension of spheres. Proc R Soc Lond A 1973;335:355–67.
[82] Davis RH. The effective thermal conductivity of a composite material with spherical inclusions. Int J Thermophys 1986;7:609–20.
[83] Kerner EH. The electrical conductivity of composite media. Proc Phys Soc B 1956;69:802–7.
[84] Van de Hulst HC. Light scattering by small particles. New York: John Wiley & Sons; 1957.
[85] Schwan HP, Schwarz G, Maczuk J, Pauly H. On the low-frequency dielectric dispersion of colloidal particles in electrolyte solution. J Phys Chem 1962;66:2626–35.
[86] Lamb W, Wood DM, Ashcroft NW. Optical properties of small particle composites: theories and applications. In: Garland JC, Tanner DB, editors. Electrical Transport and Optical Properties of Inhomogeneous Media. New York: American Institute of Physics; 1978. p. 240–55.
[87] Benveniste Y, Miloh T. On the effective thermal conductivity of coated short-fiber composites. J Appl Phys 1991;69:1337–44.
[88] Lu SY, Song JL. Effective conductivity of composites with spherical inclusions: Effective of coating and detachment. J Appl Phys 1996;79:609–18.
[89] Benveniste Y. Effective thermal conductivity of composites with a thermal contact resistance between the constituents: nondilute case. J Appl Phys 1987;61:2840–3.
[90] Hasselman DPH, Johnson LF. Effective thermal conductivity of composites with interfacial thermal barrier resistance. J Compos Mater 1987;21: 508–15.
[91] Yu W, Choi SUS. The role of interfacial layers in the enhanced thermal conductivity of nanofluids: a renovated Maxwell model. J Nanopart Res 2003;5:167–71.
[92] Yu W, Choi SUS. The role of interfacial layers in the enhanced thermal conductivity of nanofluids: a renovated Hamilton–Crosser model. J Nanopart Res 2004;6:355–61.
[93] Xie H, Fujii M, Zhang X. Effect of interfacial nanolayer on the effective thermal conductivity of nanoparticle–fluid mixture. Int J Heat Mass Transfer 2005;48:2926–32.
[94] Ren Y, Xie H, Cai A. Effective thermal conductivity of nanofluids containing spherical nanoparticles. J Phys D Appl Phys 2005;38:3958–61.
[95] Xuan Y, Li Q. Investigation on convective heat transfer and flow features of nanofluids. J Heat Transfer 2003;125:151–5.
[96] Jang SP, Choi SUS. Role of Brownian motion in the enhanced thermal conductivity of nanofluids. Appl Phys Lett 2004;84:4316–8.
[97] Koo J, Kleinstreuer C. A new thermal conductivity model for nanofluids. J Nanopart Res 2004;6:577–88.
[98] Prasher R, Bhattacharya P, Phelan PE. Thermal conductivity of nanoscale colloidal solutions (Nanofluids). Phys Rev Lett 2005;94(2) (025901).
[99] Prasher R, Bhattacharya P, Phelan PE. Brownian-motion-based convective-conductive model for the thermal conductivity of nanofluids. J Heat Transfer 2006;128:588–95.
[100] Wang BX, Zhou LP, Peng XF. A fractal model for predicting the effective thermal conductivity of liquid with suspension of nanoparticles. Int J Heat Mass Transfer 2003;46:2665–72.
[101] Prasher R, Phelan PE, Bhattacharya P. Effect of aggregation kinetics on the thermal conductivity of nanoscale colloidal solutions (Nanofluid). Nano Letters 2006;6:1529–34.
[102] Xuan Y, Li Q. Heat transfer enhancement of nanofluids. Int J Heat Mass Transfer 2000;21:58–64.
[103] Zhang X, Gu H, Fujii M. Effective thermal conductivity and thermal diffusivity of nanofluids containing spherical and cylindrical nanoparticles. J Appl Phys 2006;100:1–5 (044325).
[104] Kestin J, Wakeham WA. A contribution to the theory of the transient hot-wire technique for thermal conductivity measurements. Physica A 1978;92:102–16.
[105] Nagasaka Y, Nagashima A. Absolute measurement of the thermal conductivity of electrically conducting liquids by the transient hot-wire method. J Phys E Sci Instrum 1981;14:1435–40.
[106] Das SK, Putta N, Thiesen P, Roetzel W. Temperature dependence of thermal conductivity enhancement for nanofluids. ASME Trans J Heat Transfer 2003;125:567–74.
[107] Roetzel W, Prinzen S, Xuan Y. Measurement of thermal diffusivity using temperature oscillations. In: Cremers C, Fine H, editors. Thermal Conductivity, 21. New York/London: Plenum Press; 1990. p. 201–7.
[108] Czarnetzki W, Roetzel W. Temperature oscillation techniques for simultaneous measurement of thermal diffusivity and conductivity. Int J Thermophys 1995;16(2):413–22.
[109] Li CH, Peterson GP. Experimental investigation of temperature and volume fraction variations on the effective thermal conductivity of nanoparticle suspensions (Nanofluids). J Appl Phys 2006;99:1–8 (084314).
[110] Pak B, Cho YI. Hydrodynamic and heat transfer study of dispersed fluids with submicron metallic oxide particle. Exp Heat Transfer 1998;11:151–70.
[111] Masuda H, Ebata A, Teramae K, Hishinuma N. Alteration of thermal conductivity and viscosity of liquid by dispersing ultra-fine particles (dispersion of γ-Al_2O_3, SiO_2, and TiO_2 ultra-fine particles). Netsu Bussei 1993;7:227–33.
[112] Choi SUS, Zhang ZG, Yu W, Lockwood FE, Grulke EA. Anomalously thermal conductivity enhancement in nanotube suspensions. Appl Phys Lett 2001;79:2252–4.
[113] Eastman JA, Choi SUS, Li S, Yu W, Thompson LJ. Anomalously increased effective thermal conductivity of ethylene glycol-based nanofluids containing copper nanoparticles. Appl Phys Lett 2001;78:718–20.
[114] Xie H, Wang J, Xi T, Ai F. Thermal conductivity enhancement of suspensions containing nanosized alumina particles. J Appl Phys 2002;91:4568–72.
[115] Xie H, Lee H, Youn W, Choi M. Nanofluids containing multiwalled carbon nanotubes and their enhanced thermal conductivities. J Appl Phys 2003;94:4967–71.
[116] Wen D, Ding Y. Experimental investigation into convective heat transfer of nanofluids at the entrance region under laminar flow conditions. Int J Heat Mass Transfer 2004;47:5181–8.
[117] Wen D, Ding Y. Effective thermal conductivity of aqueous suspensions of carbon nanotubes (carbon nanotube nanofluids). J Thermophys Heat Transfer 2004;18:481–5.
[118] Liu MS, Lin MCC, Huang IT, Wang CC. Enhancement of thermal conductivity with carbon nanotube for nanofluids. Int Commun Heat Mass Transfer 2005;32:1202–10.
[119] Marquis FDS, Chibante LPF. Improving the heat transfer of nanofluids and nanolubricants with carbon nanotubes. J Minerals Metals Mater Soc 2005;57(12):32–43.
[120] Wen D, Ding Y. Formulation of nanofluids for natural convective heat transfer applications. Int J Heat Fluid Flow 2005;26:855–64.
[121] Chopkar M, Das PK, Manna I. Synthesis and characterization of a nanofluid for advanced heat transfer applications. Scr Mater 2006;55:549–52.
[122] Ding Y, Alias H, Wen D, Williams RA. Heat transfer of aqueous suspensions of carbon nanotubes (CNT nanofluids). Int J Heat Mass Transfer 2006;49: 240–50.
[123] Wen D, Ding Y. Natural convective heat transfer of suspensions of titanium dioxide nanoparticles (nanofluids). IEEE Trans Nanotechnol 2006;5:220–7.
[124] Yang Y, Grulke EA, Zhang ZG, Wu G. Thermal and rheological properties of carbon nanotube-in-oil dispersions. J Appl Phys 2006;99(8) (114307).
[125] Kang HU, Kim SH, Oh JM. Estimation of thermal conductivity of nanofluid using experimental effective particle volume. Exp Heat Transfer 2006;19:181–91.
[126] Lee D, Kim JW, Kim BG. A new parameter to control heat transport in nanofluids: surface charge state of the particle in suspension. J Phys Chem B 2006;110:4323–8.
[127] Chon CH, Kihm KD, Lee SP, Choi SUS. Empirical correlation finding the role of temperature and particle size for nanofluid (Al_2O_3) thermal conductivity enhancement. Appl Phys Lett 2005;87(3) (153107).
[128] Bhattacharya P, Saha SK, Yadav A, Phelan PE, Prasher RS. Determining the effective thermal conductivity of a nanofluid using Brownian dynamics simulation. In: Proceedings of HT2003 ASME Summer Heat Transfer Conference, Las Vegas, Nevada, USA. 2003.
[129] Xie H, Wang J, Xi T, Liu Y. Thermal conductivity of suspensions containing nanosized SiC particles. Int J Thermophys 2002;23:571–80.
[130] Xie H, Wang J, Xi T, Liu Y, Ai F. Dependence of the thermal conductivity of nanoparticle-fluid mixture on the base fluid. J Mater Sci Lett 2002;21:1469–71.
[131] Patel HE, Das SK, Sundararajan T, Nair AS, George B, Pradeep T. Thermal conductivity of naked and monolayer protected metal nanoparticle based nanofluids: manifestation of anomalous enhancement and chemical effects. Appl Phys Lett 2003;83:2931–3.
[132] Assael MJ, Metaxa IN, Arvanitidis J, Christofilos D, Lioutas C. Thermal conductivity enhancement in aqueous suspensions of carbon multi-walled and double-walled nanotubes in the present of two different dispersants. Int J Thermophys 2005;26:647–64.
[133] Evans W, Fish J, Keblinski P. Role of Brownian motion hydrodynamics on nanofluid thermal conductivity. Appl Phys Lett 2006;88:1–3 (093116).
[134] Nie C, Marlow WH, Hassan YA. Discussion of proposed mechanisms of thermal conductivity enhancement in nanofluids. Int J Heat Mass Transfer 2008;51:1342–8.
[135] Keblinski P. Mechanisms of heat flow in suspensions of nano-sized particles (Nanofluids). Int J Heat Mass Transfer 2002;45:855–63.
[136] Eastman JA, Phillpot SR, Choi SUS, Keblinski P. Thermal transport in nanofluids. Annu Rev Mater Res 2004;34:219–46.
[137] Koo J, Kleinstreuer C. Impact analysis of nanoparticle motion mechanisms on the thermal conductivity of nanofluids. Int Commun Heat Mass Transfer 2005;32:1111–8.

[138] Yu CJ, Richter AG, Datta A, Durbin MK, Dutta P. Observation of molecular layering in thin liquid films using X-ray reflectivity. Phys Rev Lett 1999;82:2326–9.
[139] Ding Y, Wen D. Particle migration in a flow of nanoparticle suspensions. Powder Technol 2005;149:84–92.
[140] Prasher R, Song D, Wang J. Measurements of nanofluid viscosity and its implications for thermal applications. Appl Phys Lett 2006;89:1–3 (133108).
[141] Li JM, Li ZL, Wang BX. Experimental viscosity measurements for copper oxide nanoparticle suspensions. Tsinghua Sci Technol 2002;7:198–201.
[142] Chen H, Ding Y, He Y, Tan C. Rheological behaviour of ethylene glycol based titania nanofluids. Chem Phys Lett 2007;444:333–7.
[143] Guo S, Luo Z, Wang T, Zhao J, Cen K. Viscosity of monodisperse silica nanofluids. Bull Chin Ceram Soc 2006;25:52–5 (in Chinese).
[144] Nguyen CT, Desgranges F, Roy G, Galanis N. Temperature and particle size dependent viscosity data for water-based nanofluid-hysteresis phenomenon. Int J Heat Fluid Flow 2007;28:1492–506.
[145] Das SK, Putra N, Roetzel W. Pool boiling characteristics of nanofluids. Int J Heat Mass Transfer 2003;46:851–62.
[146] Lee J, Hwang K, Janga S, Lee B, Kim J, Choi SUS, et al. Effective viscosities and thermal conductivities of aqueous nanofluids containing low volume concentrations of Al_2O_3 nanoparticles. Int J Heat Mass Transfer 2008;51:2651–6.
[147] Kole M, Dey TK. Viscosity of alumina nanoparticles dispersed in car engine coolant. Exp Therm Fluid Sci 2010;34:677–83.
[148] Kwak K, Kim C. Viscosity and thermal conductivity of copper oxide nanofluid dispersed in ethylene glycol. Korea Austr Rheol J 2005;17(2):35–40.
[149] Zhou SQ, Ni R. Measurement of the specific heat capacity of water-based Al_2O_3 nanofluid. Appl Phys Lett 2008;92 (093123), 3 p.
[150] He QB, Tong MW, Liu YD. Measurement of specific heat of TiO_2–$BaCl_2$–H_2O nanofluids with DSC. Refrig Air Cond 2007;7(4):19–22 (Chinese).
[151] Peng XF, Yu XL, Yu FQ. Experimental study on the specific heat of nanofluids. J Mater Sci Eng 2007;25(5):719–22 (Chinese).
[152] Wang BX, Zhou LP, Peng XF. Surface and size effects on the specific heat capacity of nanoparticles. Int J Thermophys 2006;27(1):139–51.
[153] Zhou LP, Wang BX, Peng XF, Du XZ, Yang YP. On the specific heat capacity of CuO nanofluid. Adv Mech Eng 2010;10, 1155 (172085) 4 p.
[154] Tzeng SC, Lin CW, Huang KD. Heat transfer enhancement of nanofluids in rotary blade coupling of Four-Wheel-Drive vehicles. Acta Mech 2005;179:11–23.
[155] Chein R, Huang G. Analysis of microchannel heat sink performance using nanofluids. Appl Therm Eng 2005;25:3104–14.
[156] Koo J, Kleinstreuer C. Laminar nanofluid flow in micro heat-sinks. Int J Heat Mass Transfer 2005;48:2652–61.
[157] Wong KV, De Leon O. Applications of nanofluids: current and future (review article). Adv Mech Eng 2010;10, 1155 (519659) 11 p.
[158] Putra N, Roetzel W, Das SK. Natural convection of nano-fluids. Heat Mass Transfer 2003;39(8–9):775–84.
[159] Khanafer K, Vafai K, Lightstone M. Buoyancy-driven heat transfer enhancement in a two-dimensional enclosure utilizing nanofluids. Int J Heat Mass Transfer 2003;46:3639–53.
[160] Li Q, Xuan YM. Convective heat transfer and flow characteristics of Cu–water nanofluids. Sci China Ser E 2002;45:408–16.
[161] Xuan YM, Li Q. Investigation on convective heat transfer and flow features of nanofluids. J Heat Transfer 2003;125:151–5.
[162] Lee S, Choi SUS. Application of metallic nanoparticle suspensions in advanced cooling systems. Atlanta, USA: International Mechanical Engineering Congress and Exhibition; 1996.
[163] Jang SP, Choi SUS. Cooling performance of a microchannel heat sink with nanofluids. Appl Therm Eng 2006;26:2457–63.
[164] Xuan YM, Roetzel W. Conceptions for heat transfer correlation of nanofluids. Int J Heat Mass Transfer 2000;43:3701–7.
[165] Pak BC, Cho YI. Hydrodynamic and heat transfer study of dispersed fluids with submicron metallic oxide particles. Exp Heat Transfer 1998;11:150–70.
[166] Lee J, Mudawar I. Assessment of the effectiveness of nanofluids for single phase and two-phase heat transfer in micro-channels. Int J Heat Mass Transfer 2007;50:452–63.
[167] Chein R, Chuang J. Experimental microchannel heat sink performance studies using nanofluids. Int J Therm Sci 2007;46:57–66.
[168] Yang Y, Zhong ZG, Grulke EA, Anderson WB, Wu G. Heat transfer properties of nanoparticle-in-fluid dispersion (Nanofluids) in laminar flow. Int J Heat Mass Transfer 2005;48:1107–16.
[169] Abu-Nada E. Application of nanofluids for heat transfer enhancement of separated flows encountered in a backward facing step. Int J Heat Mass Transfer 2008;29:242–9.
[170] Al-aswadi AA, Mohammed HA, Shuaib NH, Campo A. Laminar forced convection flow over a backward facing step using nanofluids. Int Commun Heat Mass Transfer 2010;37(8):945–1174.
[171] H. A. Mohammed, A. A. Al-aswadi, H. I. Abu-Mulaweh, N.H. Shuaib, Influence of nanofluids on mixed convective heat transfer over a horizontal backward facing step, In press- Heat Transfer Asian Research, March 2011.
[172] H. A. Mohammed, A. A. Al-aswadi, N.H. Shuaib, R. Saidur, Mixed convective flows over backward facing step in a vertical duct using various nanofluids- buoyancy-assisting case, In press-Thermophysics Aeromechanics, March 2011.